Chapter 9
Symmetry Approach to Chiral Optomagnonics in Antiferromagnetic Insulators

Igor Proskurin and Robert L. Stamps

Abstract We discuss several aspects of chiral optomagnonics in antiferromagnetic insulators by considering common symmetries between the electromagnetic field and spin excitations. This approach allows us to look at optical and magnetic materials from similar perspectives, and discuss useful analogies between them. We show that spin waves in collinear antiferromagnets and the electromagnetic field in vacuum are both invariant under the same eight-dimensional algebra of symmetry transformations. By such analogy, we can extend the concept of optical chirality to antiferromagnetic insulators, and demonstrate that the spin-wave dynamics in these materials in the presence of a spin current is similar to that of the light inside chiral metamaterials. Photo-excitation of magnonic spin currents is also discussed from the symmetry point of view. It is demonstrated that a direct magnonic spin photocurrent can be exited by circularly polarized light, which can be considered as a magnonic analogue of the photogalvanic effect. We also note that the *Zitterbewegung* process should appear and may play a role in photo-excitation processes.

9.1 Introduction

Modern spintronics is now a well-developed area that aims at bringing new functionality to conventional electronics by making use of the spin degrees of freedom [1], which may help to overcome looming saturation of Moore's Law [2]. There are a number of different trends in the development of the spintronics today. Among different materials, antiferromagnets play an important role, which brings us to the

I. Proskurin (✉) · R. L. Stamps
Department of Physics & Astronomy, University of Manitoba, Winnipeg R3T 2N2, Canada
e-mail: Igor.Proskurin@umanitoba.ca

R. L. Stamps
e-mail: Robert.Stamps@umanitoba.ca

I. Proskurin
Institute of Natural Sciences and Mathematics, Ural Federal University,
Ekaterinburg 620002, Russia

E. Kamenetskii (ed.), *Chirality, Magnetism and Magnetoelectricity*,
Topics in Applied Physics 138,
https://doi.org/10.1007/978-3-030-62844-4_9

field of antiferromagnetic spintronics [3, 4]. Their abundance in Nature and zero net magnetization make antiferromagnets potentially useful for applications, while the existence of two or more magnetic sublattices allows one to explore various topological effects [4]. The focus on optical manipulation of the spin states in magnetic insulators constitutes the scope of the optospintronics [5]. A prominent direction in optospintronics is related to the application of microwave cavity resonators [6], which has already seen a rapid development during the last several years [7].

Being interdisciplinary, spintronics in general, and optomagnonics in particular, can benefit by looking at the concept of chirality. Chirality or handedness, which according to the original definition given by Lord Kelvin in his Baltimore Lectures is related to the lack of symmetry between an object and its mirror image [8]. It is a universal phenomenon that has proved its significance in various scientific areas from high-energy physics to life sciences and soft matter [9]. Kelvin's definition, which is purely geometric, was generalized later to accommodate dynamical phenomena by Barron [10]. Thus, according to Barron's definition, one should distinguish between *true* and *false* chiralities. The former is to be found in the systems that break inversion symmetry, but at the same time are invariant under a time-reversal transformation combined with any proper rotation, while the latter is characterized by breaking time-reversal and inversion symmetries simultaneously [11].

How can the concept of chirality be useful for the development of optospintronics? A general observation is that the goal of the spintronics is manipulation and transformation of pure spin currents, and spin currents are chiral. Indeed, in agreement with the definition of true chirality, a flow of angular momentum reverses its sign under spatial inversion, while it remains invariant under the time reversal transformation, which reverses both velocities and spins. Thus, from the symmetry point of view, pure spin currents are in the same category as, for example, natural optical activity and circular dichroism in optics. This argument also suggests that materials with structural chirality may have unique properties for hosting and transferring spin currents that makes them interesting for applications, which is reflected in the rapid development of molecular spintronics [12, 13] and related topics such as chiral spin selectivity [14].

Another observation helpful to establish a link between optics and spintronics is that not only geometric structures but also physical fields can be characterized by chirality. Chirality density of the electromagnetic field, for example, has been known for a long time. Lipkin first noticed that the Maxwell's equations in vacuum have a hidden conservation law for a chiral density, which he dubbed *zilch* due to the lack of clear physical meaning of this quantity at that time [15]. Later, it was demonstrated that this conservation law is closely related to electromagnetic duality [16, 17]. This eventually led to the formulation of the *nongeometric* symmetries of the Maxwell's equations [18], i. e. the symmetries, which are not reduced to space-time transformations. For several decades, the formal properties of optical chirality, helicity, and dual symmetries were discussed [19–26] but it was not until Tang and Cohen showed how electromagnetic chirality density can be used to characterize dichroism in light interacting with a chiral metamaterial that this was understood for materials [27]. This revived interest in optical chirality [28–31], which has found a number of applications in optics and plasmonics [32–37].

The results of Tang and Cohen [27] can be understood as follows. In order to observe effects related to the chirality of light, we have to put the electromagnetic field in contact with a chiral environment. This principle suggests a way for finding similar effects in other systems. For example, spin-wave dynamics in collinear antiferromagnets can be represented in a form that closely resembles the Silberstein-Bateman formulation of the Maxwell's equations. Since collinear antiferromagnets have two magnetic sublattices, the concept of electromagnetic duality and nongeometric symmetries can be generalized to transformations between the antiferromagnetic sublattices [38]. This allows to establish a conservation law for a spin-wave analogue of the optical chirality. Injection of a spin current into the antiferromagnet in this case has an effect similar to a chiral environment for light-matter interactions inside a metamaterial [38].

It is also remarkable that both the Maxwell's equations [39] and the dynamics of antiferromagnetic spin waves [40] allow a formulation in the form of the Dirac equation for an ultra-relativistic particle. Such particles are characterized by conserving helicity—a projection of spin on the linear momentum [41], which also satisfies the definition of true chirality. Breaking the symmetry between right and left, in this case, corresponds to a Weyl material [42], wherein quasi-particles with different helicities are spatially separated. Symmetry considerations suggest that as far as single particle dynamics is concerned, there should be some analogy between optical metamaterials, Weyl semimetals, and chiral antiferromagnets. There has been several proposals in these directions. For example, one can emulate the chiral magnetic effect in metallic antiferromagnets [43].

These arguments have a direct impact on optospintronics. Since optical chirality and spin currents share the same symmetry properties, it is possible to use polarized light to excite magnon spin-photocurrents in antiferromagnetic insulators [44]. Circular polarized light in this case creates a direct *flow* of magnon angular momentum, whose direction is controlled by helicity of light. This effect resembles the circular photogalvanic effect in metals [45], which recently attracted attention in topological electron materials [46]. It has been demonstrated that for a separated Weyl node, the photocurrent excitation rate is determined by the product of the topological charge of the node and the helicity of light [46].

In this Chapter, we review chiral excitations in optics and antiferromagnetic insulators together with their applications in optomagnonics. Our discussion is organized as follows. In Sect. 9.2, we give a brief review of optical chirality and nongeometric symmetries, which is generalized to antiferromagnetic spin-waves in Sect. 9.3, where we discuss potential applications such as spin-current induced magnon dichroism. Section 9.4 is reserved for photo-excitation of magnon spin currents with polarized light. Summary and conclusions are in Sect. 9.5.

9.2 Optical Chirality and Nongeometric Symmetries of the Maxwell's Equations

Since the early developments of electrodynamics, it has been well established that the electromagnetic field in vacuum can be characterized by conserving energy, momentum, angular momentum, which reflects the invariance of the Maxwell's equations with respect to the translations and rotations in the four-dimensional space-time [18]. It was found almost by chance [15] that in addition to these conservation laws, the electromagnetic field has another invariant given by a combination of the electric, $\boldsymbol{E}$, and magnetic, $\boldsymbol{B}$, fields

$$\rho_\chi(t, \boldsymbol{r}) = \frac{\varepsilon_0}{2}\boldsymbol{E}\cdot(\nabla\times\boldsymbol{E}) + \frac{1}{2\mu_0}\boldsymbol{B}\cdot(\nabla\times\boldsymbol{B}), \tag{9.1}$$

which is odd under the spatial inversion and even under the time reversal transformations (ε_0 and μ_0 are the vacuum permittivity and permeability respectively). For this quantity, Lipkin coined a special term—optical *zilch* to emphasize the lack of a clear physical interpretation at that time [15]. According to its symmetry properties, ρ_χ is *truly chiral* [10], and can be considered as a chirality density of the electromagnetic field.

Using the Maxwell's equations, it is straightforward to demonstrate that in vacuum ρ_χ satisfies the continuity equation

$$\frac{\partial\rho_\chi}{\partial t} + \nabla\cdot\boldsymbol{J}_\chi = 0, \tag{9.2}$$

where

$$\boldsymbol{J}_\chi(t, \boldsymbol{r}) = \frac{\varepsilon_0}{2}\boldsymbol{E}\times\frac{\partial\boldsymbol{E}}{\partial t} + \frac{1}{2\mu_0}\boldsymbol{B}\times\frac{\partial\boldsymbol{B}}{\partial t}, \tag{9.3}$$

determines the corresponding zilch flow.

In this section, we will show that this conservation law belongs to the class of so-called "hidden" or *nongeometric* symmetries of the Maxwell's equations. One of these symmetries, which has been known since the time of Heaviside, Larmor, and Rainich, is the duality symmetry [47, 48]. If we consider Maxwell's equations in free space

$$\nabla\times\boldsymbol{E} = 0, \qquad \nabla\times\boldsymbol{B} = 0, \tag{9.4}$$

$$\nabla\cdot\boldsymbol{E} = 0, \qquad \nabla\cdot\boldsymbol{B} = 0, \tag{9.5}$$

(we set $c = 1$ throughout this section) the electromagnetic duality is a symmetry with respect to the rotation in the pseudo-space of the electric and magnetic fields, which leaves Maxwell's equations invariant

$$\boldsymbol{E} \to \boldsymbol{E}' = \boldsymbol{E}\cos\theta + \boldsymbol{B}\sin\theta, \tag{9.6}$$

$$\boldsymbol{B} \to \boldsymbol{B}' = -\boldsymbol{E}\sin\theta + \boldsymbol{B}\cos\theta, \tag{9.7}$$

where θ is a real parameter of the transformation. This symmetry is usually broken inside materials, unless we deal with a dual symmetric medium [49].

The existence of duality symmetry guarantees the conservation of optical helicity, i. e. the projection of spin angular momentum of the photon onto its linear momentum [16, 17, 23, 24]. It should be mentioned, however, that the formulation of helicity conservation law in classical electrodynamics is not straightforward, because the standard Lagrangian for the electromagnetic field is not dual symmetric [48]. Using the dual symmetric representation for the electromagnetic Lagrangian combined with the Noether's approach, it is possible to express the optical helicity density in the form similar to (9.1)

$$\rho_{\text{hel}}(t, \boldsymbol{r}) = \frac{1}{2}\left[\boldsymbol{A}\cdot(\nabla\times\boldsymbol{A}) + \boldsymbol{C}\cdot(\nabla\times\boldsymbol{C})\right], \tag{9.8}$$

where in addition to the magnetic vector potential $\boldsymbol{A}$, we also introduced the electric vector potential $\boldsymbol{C}$, which satisfies the following equations, $\boldsymbol{E} = -\nabla\times\boldsymbol{C} = -\partial_t\boldsymbol{A}$ and $\boldsymbol{B} = \nabla\times\boldsymbol{A} = \partial_t\boldsymbol{C}$. These are invariant under the transformations in (9.6) and (9.7) [47, 48].

The definition of electromagnetic helicity depends on a specific representation of the Lagrangian. It suggests that it would be useful to have a general formalism for deriving "hidden" symmetries and conservation laws directly from the equations of motion formulated exclusively in terms of the electromagnetic fields, and independent of any gauge choice. Such a formalism has been developed by Fushchich and Nikitin [18]. Below, we give a brief review of this formalism, which is necessary for further discussions.

9.2.1 Symmetry Analysis of the Maxwell's Equations

For the symmetry analysis, it is convenient to formulate Maxwell's equations in the form that resembles the Dirac equation for a massless relativistic particle. This representation is called the Silberstein-Bateman form [18]. In this form, the first pair of the Maxwell's equations in (9.4) is rewritten in terms of a Schrödinger-like equation for the six-component vector column composed of the components of the electric and magnetic fields $\phi = (\boldsymbol{E}, \boldsymbol{B})^T$

$$i\frac{\partial\phi(t, \boldsymbol{p})}{\partial t} = \mathcal{H}(\boldsymbol{p})\phi(t, \boldsymbol{p}), \tag{9.9}$$

where for convenience, we work in the momentum space, $\boldsymbol{p}$, defined by the following Fourier transformations

$$\boldsymbol{E}(t,\boldsymbol{r}) = \frac{1}{(2\pi)^{3/2}}\int d^3p e^{i\boldsymbol{p}\cdot\boldsymbol{r}}\boldsymbol{E}(t,\boldsymbol{p}), \tag{9.10}$$

$$\boldsymbol{B}(t,\boldsymbol{r}) = \frac{1}{(2\pi)^{3/2}}\int d^3p e^{i\boldsymbol{p}\cdot\boldsymbol{r}}\boldsymbol{B}(t,\boldsymbol{p}). \tag{9.11}$$

The matrix on the right-hand side of equation (9.9) has the following structure

$$\mathcal{H}(\boldsymbol{p}) = \begin{pmatrix} 0 & i(\hat{\boldsymbol{S}}\cdot\boldsymbol{p}) \\ -i(\hat{\boldsymbol{S}}\cdot\boldsymbol{p}) & 0 \end{pmatrix}, \tag{9.12}$$

which can be considered as a direct product of the Pauli matrix σ_2, which interchanges $\boldsymbol{E}$ and $\boldsymbol{B}$, and the "helicity" operator $(\hat{\boldsymbol{S}}\cdot\boldsymbol{p})$, where the matrices $\hat{S}_\alpha$ $(\alpha = x, y, z)$ form a representation of the three-dimensional rotation group, $(\hat{S}_\alpha)_{\beta\gamma} = i\epsilon_{\alpha\beta\gamma}$, with $\epsilon_{\alpha\beta\gamma}$ being the Levi-Civita symbol.

The second pair of the Maxwell's equations (9.5) in this formalism impose an additional constraint on the components of $\phi(t,\boldsymbol{p})$ [18]

$$(\hat{\boldsymbol{S}}\cdot\boldsymbol{p})^2\phi(t,\boldsymbol{p}) = p^2\phi(t,\boldsymbol{p}), \tag{9.13}$$

which acknowledges transversality of the electromagnetic field in vacuum.

9.2.1.1 Invariance Algebra of the Maxwell's Equations

Now, we can find the symmetry operations that transform a solution $\phi(t,\boldsymbol{p})$ of (9.9) into another solution $\tilde{\phi}(t,\boldsymbol{p}) = Q(\boldsymbol{p})\phi(t,\boldsymbol{p})$. We look for these transformations in the form of the six-dimensional matrices $Q(\boldsymbol{p})$, which may depend on the momentum $\boldsymbol{p}$. Formal resemblance of our representation with the quantum mechanics implies that these matrices should commute with $\mathcal{H}(\boldsymbol{p})$.

The problem of finding all such transformation becomes almost trivial if we transform to the helicity basis, where $\mathcal{H}(\boldsymbol{p})$ is diagonal. This transformation is reached by a combination of the rotation in the three-dimensional space

$$\hat{U}_\Lambda = \begin{pmatrix} -\dfrac{p_xp_z + ip_yp}{\sqrt{2}pp_\perp} & \dfrac{p_xp_z - ip_yp}{\sqrt{2}pp_\perp} & \dfrac{p_x}{p} \\ -\dfrac{p_yp_z - ip_xp}{\sqrt{2}pp_\perp} & \dfrac{p_yp_z + ip_xp}{\sqrt{2}pp_\perp} & \dfrac{p_y}{p} \\ \dfrac{p_\perp}{\sqrt{2}p} & -\dfrac{p_\perp}{\sqrt{2}p} & \dfrac{p_z}{p} \end{pmatrix}, \tag{9.14}$$

where $p_\perp = (p_x^2 + p_y^2)^{1/2}$, which diagonalizes the "helicity" operator, $\hat{U}_\Lambda^\dagger(\hat{\boldsymbol{S}}\cdot\boldsymbol{p})\hat{U}_\Lambda = \mathrm{diag}(-p, p, 0)$ (it transforms to the basis where the electric and magnetic fields are written in terms of circularly polarized components), with the $SU(2)$ transformation in the pseudo-space of electric and magnetic fields

$$U_2 = \frac{1}{\sqrt{2}} \begin{pmatrix} 1 & -i \\ -i & 1 \end{pmatrix}. \tag{9.15}$$

The resulting transformation $\mathcal{U} = U_2 \otimes \hat{U}_\Lambda$ diagonalizes $\mathcal{H}(\boldsymbol{p})$ so that in the transformed frame

$$\tilde{\mathcal{H}} = \mathcal{U}^\dagger \mathcal{H} \mathcal{U} = \mathrm{diag}(-p, p, 0, p, -p, 0). \tag{9.16}$$

The eigenvalues of $\tilde{\mathcal{H}}$ correspond to the left and right polarized electromagnetic modes with the linear frequency dispersion cp (we have recovered the speed of light c here), which are degenerate in the absence of light-matter interactions.

Straightforward calculations show that in the diagonal frame, any matrix that commutes with $\tilde{\mathcal{H}}$, and at the same time leaves (9.13) invariant, is parameterized by eight parameters, $a, \ldots h$, and has the following structure

$$\tilde{Q} = \begin{pmatrix} a & 0 & 0 & 0 & e & 0 \\ 0 & b & 0 & f & 0 & 0 \\ 0 & 0 & 0 & 0 & 0 & 0 \\ 0 & g & 0 & c & 0 & 0 \\ h & 0 & 0 & 0 & d & 0 \\ 0 & 0 & 0 & 0 & 0 & 0 \end{pmatrix}. \tag{9.17}$$

The basis in the linear space of $\tilde{Q}$ can be chosen such as its basis elements, $\tilde{Q}_i$, ($i = 1, \ldots, 8$) form the algebra isomorphic to the Lie algebra of the group $U(2) \otimes U(2)$

$$\begin{aligned} &\tilde{Q}_1 = -\sigma_2 \otimes \hat{S}_y, && \tilde{Q}_2 = -i\sigma_3 \otimes \hat{I} \\ &\tilde{Q}_3 = -i\sigma_1 \otimes \hat{S}_y, && \tilde{Q}_4 = \sigma_1 \otimes \hat{S}_x \\ &\tilde{Q}_5 = -\sigma_0 \otimes \hat{S}_z, && \tilde{Q}_6 = \sigma_2 \otimes \hat{S}_x \\ &\tilde{Q}_7 = \sigma_0 \otimes \hat{I}, && \tilde{Q}_8 = i\sigma_3 \otimes \hat{S}_z, \end{aligned} \tag{9.18}$$

where σ_0 and $\hat{I}$ denote 2×2 and 3×3 unit matrices respectively.

Returning into original frame and taking into account that $\hat{U}_\Lambda \hat{S}_z \hat{U}_\Lambda^\dagger = -(\hat{\boldsymbol{S}} \cdot \boldsymbol{p})/p$, we obtain the generators of the symmetry transformations in the following form

$$\begin{aligned} &Q_1 = \sigma_3 \otimes (\hat{\boldsymbol{S}} \cdot \tilde{\boldsymbol{p}})\hat{D}, && Q_2 = i\sigma_2 \otimes \hat{I}, \\ &Q_3 = -\sigma_1 \otimes (\hat{\boldsymbol{S}} \cdot \tilde{\boldsymbol{p}})\hat{D}, && Q_4 = -\sigma_1 \otimes \hat{D}, \\ &Q_5 = \sigma_0 \otimes (\hat{\boldsymbol{S}} \cdot \tilde{\boldsymbol{p}}), && Q_6 = -\sigma_3 \otimes \hat{D}, \\ &Q_7 = \sigma_0 \otimes \hat{I}, && Q_8 = i\sigma_2 \otimes (\hat{\boldsymbol{S}} \cdot \tilde{\boldsymbol{p}}), \end{aligned} \tag{9.19}$$

where $\tilde{\boldsymbol{p}} = \boldsymbol{p}/p$, and $\hat{D} = -p\hat{U}_\Lambda \hat{S}_x \hat{U}_\Lambda^\dagger$. These equations form the eight-dimensional invariance algebra of the Maxwell's equations in vacuum [18].

9.2.1.2 Nongeometric Symmetries

The basis elements in (9.19) generate continuous symmetries that Fushchich and Nikitin called the *nongeometric symmetries* of the Maxwell's equations [18]

$$\phi(t, \boldsymbol{p}) \rightarrow \phi'(t, \boldsymbol{p}) = \exp(Q_i\theta_i)\phi(t, \boldsymbol{p}), \tag{9.20}$$

where θ_i denotes the real parameter of the transformation.

Some symmetry generators have a clear physical meaning. For example, Q_7 is a unit element. Q_2 interchanges electric and magnetic fields in $\phi(t, \boldsymbol{p})$, so that the corresponding continuous transformation $\exp(i\sigma_2\theta)$ is the duality symmetry in (9.6) and (9.7). Q_5 has the form of the helicity operator. Q_8 is proportional to $\mathcal{H}$, which means that similar to Q_7 it commutes with every element of the algebra. It reflects the symmetry with respect to ∂_t (the time derivative of $\phi(t, \boldsymbol{p})$, which solves the Maxwell's equations, is again a solution for the same $\boldsymbol{p}$). The basis elements Q_2, Q_5, Q_7, and Q_8 form a trivial Abelian part of the algebra in (9.19). The existence of non-Abelian elements is related to the degeneracy between left and right polarized eigenvalues in (9.16).

The conservation laws that correspond to the symmetry transformations in (9.20) can be conveniently written in terms of the bilinear forms by analogy with the quantum-mechanics

$$\langle Q_i \rangle = \frac{1}{2}\int d^3p\phi^\dagger(t, \boldsymbol{p})Q_i\phi(t, \boldsymbol{p}). \tag{9.21}$$

It can be demonstrated that the electromagnetic field in vacuum can be characterized by an infinite number of invariants generated from the eight symmetry transformations [18]. For example, the unit element Q_7 in this formalism corresponds to the conservation of the electromagnetic energy

$$\langle Q_7 \rangle = \frac{1}{2}\int d^3p\phi^\dagger(t, \boldsymbol{p})\phi(t, \boldsymbol{p}) = \frac{1}{2}\int d^3p\left(E^2 + B^2\right). \tag{9.22}$$

9.2.1.3 Conservation Law for Optical Chirality

Using this formalism, optical zilch can be expressed as a conservation law for the helicity operator Q_5

$$C_\chi = \int d^3r\rho_\chi(t, \boldsymbol{r}) = \frac{1}{2}\int d^3p\phi^\dagger(t, \boldsymbol{p})(\hat{\boldsymbol{S}} \cdot \boldsymbol{p})\phi(t, \boldsymbol{p}). \tag{9.23}$$

Using the fact that the helicity operator, duality symmetry, and ∂_t are related to each other by the algebraic property, $pQ_5Q_2 = -i\mathcal{H} = \partial_t$, we establish a relation between zilch conservation and duality symmetry as it was originally discussed in [16, 17], which allows to write the conservation law above in the following equivalent form

$$C_\chi = -\frac{i}{2}\int d^3p\phi^\dagger(t,\boldsymbol{p})Q_2\partial_t\phi(t,\boldsymbol{p}) = \frac{1}{2}\int d^3r\left(\boldsymbol{B}\cdot\frac{\partial\boldsymbol{E}}{\partial t} - \boldsymbol{E}\cdot\frac{\partial\boldsymbol{B}}{\partial t}\right). \quad (9.24)$$

This expression can be easily generalized to accommodate higher order terms in space and time derivatives. By replacing $Q_2\partial_t$ with $-(ip)^{2n}Q_2(i\partial_t)^{2m+1}$, which is again a symmetry operation, we can find a hierarchy of conserving zilches

$$C_\chi^{(m,n)} = \frac{1}{2}\int d^3r\left(\boldsymbol{B}\cdot\nabla^{2n}\partial_t^{2m+1}\boldsymbol{E} - \boldsymbol{E}\cdot\nabla^{2n}\partial_t^{2m+1}\boldsymbol{B}\right), \quad (9.25)$$

where 00-zilch corresponds to the optical chirality [23, 24, 31].

It is possible to derive the conservation law for the optical zilch using the Noether's formalism by applying a specific "hidden" gauge transformation to the Lagrangian of the electromagnetic field [31], which leads to the same results as in (9.23) and (9.25). The advantage of the approach discussed in this section, based on the symmetry analysis of the Maxwell's equations, is that it does not depend on any specific gauge choice. This fact makes it easy to extend this formalism to other physical systems with similar form of the equations of motion.

9.2.2 *Optical Chirality in Gyrotropic Media*

Having now a complete picture of the nongeometric symmetries in vacuum, we discuss how this approach can be applied for the light-matter interactions. Electromagnetic field in dielectric medium is usually described by the material form of the Maxwell equations

$$\nabla\times\boldsymbol{E} = -\frac{\partial\boldsymbol{B}}{\partial t}, \qquad \nabla\cdot\boldsymbol{B} = 0, \quad (9.26)$$

$$\nabla\times\boldsymbol{H} = \frac{\partial\boldsymbol{D}}{\partial t}, \qquad \nabla\cdot\boldsymbol{D} = 0, \quad (9.27)$$

supplemented by the constituent relations between the fields $\boldsymbol{E}$, $\boldsymbol{H}$, $\boldsymbol{D}$, and $\boldsymbol{B}$. The constituent relations impose additional constraints on the form of the symmetry transformations for the electromagnetic field, which reflect the intrinsic symmetries of the medium. This often leads to the reduction of the invariance algebra in (9.19) to lesser number of elements [50]. In the case of common constituent relations, $\boldsymbol{D}(\boldsymbol{p}) = \hat{\varepsilon}(\boldsymbol{p})\boldsymbol{E}(\boldsymbol{p})$ and $\boldsymbol{B}(\boldsymbol{p}) = \hat{\mu}(\boldsymbol{p})\boldsymbol{H}(\boldsymbol{p})$, where $\hat{\varepsilon}(\boldsymbol{p})$ and $\hat{\mu}(\boldsymbol{p})$ denote the electric permittivity and magnetic permeability tensors in the Fourier space, Maxwell's equations in (9.9) are replaced by

$$i\frac{\partial}{\partial t}\begin{pmatrix} \boldsymbol{D}(\boldsymbol{p}) \\ \boldsymbol{B}(\boldsymbol{p}) \end{pmatrix} = \begin{pmatrix} 0 & i(\hat{\boldsymbol{S}}\cdot\boldsymbol{p})\hat{\mu}^{-1}(\boldsymbol{p}) \\ -i(\hat{\boldsymbol{S}}\cdot\boldsymbol{p})\hat{\varepsilon}^{-1}(\boldsymbol{p}) \end{pmatrix} \begin{pmatrix} \boldsymbol{D}(\boldsymbol{p}) \\ \boldsymbol{B}(\boldsymbol{p}) \end{pmatrix}. \tag{9.28}$$

The symmetry analysis of the previous sections can be generalized for this case (see [50] for detailed discussion). In particular, for dual symmetric medium, the optical chirality is given by

$$C_\chi = \frac{1}{2}\int d^3p \left(\boldsymbol{D}^*(\boldsymbol{p})(\hat{\boldsymbol{S}}\cdot\boldsymbol{p})\hat{\varepsilon}^{-1}(\boldsymbol{p})\boldsymbol{D}(\boldsymbol{p}) + \boldsymbol{B}^*(\boldsymbol{p})(\hat{\boldsymbol{S}}\cdot\boldsymbol{p})\hat{\mu}^{-1}(\boldsymbol{p})\boldsymbol{B}(\boldsymbol{p})\right) \tag{9.29}$$

In the real space this expression becomes

$$C_\chi = \frac{1}{2}\int d^3r\,(\boldsymbol{B}\cdot\partial_t\boldsymbol{D} - \boldsymbol{D}\cdot\partial_t\boldsymbol{B})\,, \tag{9.30}$$

which also acknowledges spatial dispersion of the electromagnetic field.

As an important example, let us consider propagation of the electromagnetic field in chiral media where structural chirality of the material leads to the existence of such physical phenomena as natural optical activity and circular dichroism. There exists several approaches for the electrodynamics of chiral gyrotropic media [51–53]. One of these approaches, which is frequently adopted for characterizing metamaterials [54, 55], is based on the following constituent relations

$$\boldsymbol{D} = \varepsilon\varepsilon_0\boldsymbol{E} + i\varkappa\boldsymbol{H}, \tag{9.31}$$

$$\boldsymbol{B} = \mu\mu_0\boldsymbol{H} - i\varkappa\boldsymbol{E}, \tag{9.32}$$

where $\varkappa$ characterizes chirality of the material. This approach requires complex representation for the electromagnetic fields and can be derived from the relativistic covariance principle [51, 56].

By applying our general formalism to the Maxwell's equations (9.26) and (9.27) with the constituent relations (9.31) and (9.32), we obtain the same equation of motion as in (9.9), where ϕ is replaced by for the vector column $\phi(t,\boldsymbol{p}) = (\boldsymbol{D},\boldsymbol{B})^T$, and the matrix on the right-hand side is now given by (we use the units $\varepsilon\varepsilon_0 = \mu\mu_0 = 1$)

$$\mathcal{H}(\boldsymbol{p}) = -\frac{1}{1-\varkappa^2}\begin{pmatrix} \varkappa(\hat{\boldsymbol{S}}\cdot\boldsymbol{p}) & -i(\hat{\boldsymbol{S}}\cdot\boldsymbol{p}) \\ i(\hat{\boldsymbol{S}}\cdot\boldsymbol{p}) & \varkappa(\hat{\boldsymbol{S}}\cdot\boldsymbol{p}) \end{pmatrix}. \tag{9.33}$$

This matrix can be diagonalized by a combination of the same unitary transformations as in (9.14) and (9.15) that yields the following diagonal form

$$\tilde{\mathcal{H}} = \mathcal{U}^\dagger\mathcal{H}\mathcal{U} = \mathrm{diag}(-p_-, p_-, 0, p_+, -p_+, 0), \tag{9.34}$$

where $p_\pm = p/(1\mp\varkappa)$.

Lifted degeneracy between left (p_-) and right (p_+) polarized eigenmodes in (9.34) leads to the reduction of the eight-dimensional invariance algebra to four basis elements, which commute with each other

$$\begin{aligned} Q_2 &= i\sigma_2 \otimes \hat{I},\ Q_5 = \ \ \sigma_0 \otimes (\hat{\boldsymbol{S}} \cdot \tilde{\boldsymbol{p}}) \\ Q_7 &= \ \ \sigma_0 \otimes \hat{I},\ Q_8 = i\sigma_2 \otimes (\hat{\boldsymbol{S}} \cdot \tilde{\boldsymbol{p}}). \end{aligned} \tag{9.35}$$

These symmetries, however, still contain the duality transformation Q_2, which means that the medium is dual-symmetric and supports the conservation of the electromagnetic helicity [49] and, as a consequence, optical zilches.

Definition of the optical chirality density in chiral media requires some attention. This situation is similar to the definition of the electromagnetic energy density where one should take care of the continuity of the energy flow at the boundary between two chiral media [51]. It can be demonstrated that chirality density in the medium with constituent relations (9.31) and (9.32) that provides continuity of chirality flow at the boundary of two chiral media with different $\varkappa$ can be introduced in the following way [50]

$$\rho_\chi = \frac{\varepsilon\varepsilon_0}{2}\boldsymbol{B}^* \cdot \frac{\partial \boldsymbol{E}}{\partial t} - \frac{\mu\mu_0}{2}\boldsymbol{D}^* \cdot \frac{\partial \boldsymbol{H}}{\partial t}, \tag{9.36}$$

This expression remains valid even if $\varepsilon(\boldsymbol{r})$, $\mu(\boldsymbol{r})$, and $\varkappa(\boldsymbol{r})$ become position dependent. In this case, it satisfies the continuity equation with a source term on the right-hand side

$$\partial_t \rho_\chi + \nabla \cdot \boldsymbol{J}_\chi = F(t, \boldsymbol{r}). \tag{9.37}$$

where

$$\boldsymbol{J}_\chi = \frac{\varepsilon_0\varepsilon}{2}\boldsymbol{E}^* \times \partial_t \boldsymbol{E} + \frac{\mu_0\mu}{2}\boldsymbol{H}^* \times \partial_t \boldsymbol{H}, \tag{9.38}$$

and the source term contains only gradients of ε and μ, but does not depend on the gradient of $\varkappa$

$$F(t, \boldsymbol{r}) = \frac{\varepsilon_0}{2}\nabla\varepsilon \cdot \boldsymbol{E}^* \times \partial_t \boldsymbol{E} + \frac{\mu_0}{2}\nabla\mu \cdot \boldsymbol{H}^* \times \partial_t \boldsymbol{H}. \tag{9.39}$$

In order to understand the physical meaning of ρ_χ, let us look at energy absorption in a dissipative gyrotropic medium with the constituent relations (9.31) and (9.32). As was demonstrated in [27], the electromagnetic energy absorption rate in this case has an asymmetric part, which has opposite signs for left and right polarized electromagnetic waves. This part is proportional the product between the chirality of the material, given by the imaginary part of $\varkappa$, and the chirality density of the electromagnetic field ρ_χ. The flow of optical chirality in (9.3), in this situation, can be associated with the asymmetric components of the electromagnetic forces in the medium, which can be used, for example, for optical separation of chiral molecules [37].

In the next section, we will show how these arguments can be generalized to spin excitations in antiferromagnetic materials. Similar to the results of this section, the symmetry analysis will play a principal role in our discussion.

9.3 Spin-Wave Chirality in Antiferromagnetic Insulators

The symmetry analysis developed in the previous section for Maxwell's equations can be generalized to other dynamical systems. Here, we develop such generalization for spin-wave excitations in an antiferromagnetic insulator. A key observation that helps us to draw the analogy between spin-wave dynamics and electrodynamics is that the antiferromagnetic spin waves can be also characterized by two polarization states. This stems from the fact that the magnetization dynamics in antiferromagnets involves two coupled magnetic sublattices. We, therefore, examine the symmetry transformation in the extended space that includes three-dimensional rotations and transformations between the sublattices, in order to find an algebra of nongeometric symmetries for spin waves equivalent to that of the electrodynamics.

9.3.1 Equations of Motion for Antiferromagnetic Spin Waves

We start our discussion with a simple case of a collinear antiferromagnet with two equivalent magnetic sublattices $\boldsymbol{M}_1(t, \boldsymbol{r})$ and $\boldsymbol{M}_2(t, \boldsymbol{r})$. The energy for such antiferromagnet can be written in the following form

$$W = \int d^3r \left[\frac{\alpha}{2} \left(\frac{\partial \boldsymbol{M}_1}{\partial x_\mu} \cdot \frac{\partial \boldsymbol{M}_1}{\partial x_\mu} + \frac{\partial \boldsymbol{M}_2}{\partial x_\mu} \cdot \frac{\partial \boldsymbol{M}_2}{\partial x_\mu} \right) + \alpha' \frac{\partial \boldsymbol{M}_1}{\partial x_\mu} \cdot \frac{\partial \boldsymbol{M}_2}{\partial x_\mu} \right.$$
$$\left. + \frac{\delta}{2} \boldsymbol{M}_1 \cdot \boldsymbol{M}_2 - \frac{\beta}{2} \left((\boldsymbol{M}_1 \cdot \boldsymbol{n})^2 + (\boldsymbol{M}_2 \cdot \boldsymbol{n})^2 \right) \right], \quad (9.40)$$

where α, α', and δ are the antiferromagnetic exchange parameters and $\beta > 0$ describes the uniaxial magnetic anisotropy with $\boldsymbol{n}$ being the unit vector along the anisotropy axis [57]. In the ground state, the anisotropy stabilizes a uniform magnetic ordering along $\boldsymbol{n}$ where two sublattices compensate each other, $\boldsymbol{M}_1 = -\boldsymbol{M}_2$, so that the total magnetization vanishes.

In the semi-classical limit, magnetization dynamics are described by the Landau–Lifshitz–Gilbert equations of motion

$$\frac{\partial \boldsymbol{M}_i}{\partial t} = \gamma \boldsymbol{M}_i \times \boldsymbol{H}_i^{\text{eff}} - \eta \boldsymbol{M}_i \times \frac{\partial \boldsymbol{M}_i}{\partial t}, \quad (i = 1, 2), \quad (9.41)$$

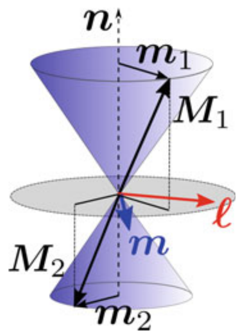

Fig. 9.1 Sublattice magnetizations $\boldsymbol{M}_1$ and $\boldsymbol{M}_2$ precessing along the anisotropy axis $\boldsymbol{n}$; $\boldsymbol{m} = \boldsymbol{m}_1 + \boldsymbol{m}_2$ is the resulting dynamic magnetization, and $\boldsymbol{l} = \boldsymbol{m}_1 - \boldsymbol{m}_2$ shows the dynamic part of the antiferromagnetic vector

where γ is the gyromagnetic ratio, $\boldsymbol{H}_i^{\rm eff} = -\delta W/\delta \boldsymbol{M}_i$ is the effective field acting on the magnetization on the ith sublattice and η is the Gilbert damping that takes dissipation into account [57].

For small excitations around the ground state configuration a linear form of the Landau–Lifshitz–Gilbert equations of can be used. This is reached by breaking the sublattice magnetizations into static $M_s\boldsymbol{n}$ and dynamic $\boldsymbol{m}_i(t, \boldsymbol{t})$ parts, $\boldsymbol{M}_i = (-1)^{i+1} M_s \boldsymbol{n} + \boldsymbol{m}_i$, and keeping only the linear terms in $\boldsymbol{m}_i$ in the resulting equations of motion (M_s denotes the saturation magnetization). For convenience, we transform $\boldsymbol{m}_i(\boldsymbol{r})$ to momentum space, such that $\boldsymbol{m}_i(t, \boldsymbol{r}) = \int d^3 p \exp(i\boldsymbol{p}\cdot\boldsymbol{r})\boldsymbol{m}_{i\boldsymbol{p}}(t)$, and introduce the dynamic vectors of the magnetization, $\boldsymbol{m}_{\boldsymbol{p}} = \boldsymbol{m}_{1\boldsymbol{p}} + \boldsymbol{m}_{2\boldsymbol{p}}$, and antiferromagnetism, $\boldsymbol{l}_{\boldsymbol{p}} = \boldsymbol{m}_{1\boldsymbol{p}} - \boldsymbol{m}_{2\boldsymbol{p}}$, see Fig. 9.1. The resulting linear system of the equations of motions is given by

$$\frac{\partial \boldsymbol{m}_{\boldsymbol{p}}}{\partial t} = -\varepsilon_{\boldsymbol{p}}^{(l)} \boldsymbol{n} \times \boldsymbol{l}_{\boldsymbol{p}} + \eta \boldsymbol{n} \times \frac{\partial \boldsymbol{l}_{\boldsymbol{p}}}{\partial t}, \tag{9.42}$$

$$\frac{\partial \boldsymbol{l}_{\boldsymbol{p}}}{\partial t} = -\varepsilon_{\boldsymbol{p}}^{(m)} \boldsymbol{n} \times \boldsymbol{m}_{\boldsymbol{p}} + \eta \boldsymbol{n} \times \frac{\partial \boldsymbol{m}_{\boldsymbol{p}}}{\partial t}, \tag{9.43}$$

where $\varepsilon_{\boldsymbol{p}}^{(m)} = \gamma M_s(\delta + \beta + (\alpha + \alpha')p^2)$ and $\varepsilon_{\boldsymbol{p}}^{(l)} = \gamma M_s(\beta + (\alpha - \alpha')p^2)$.

For the equations of motion (9.42) and (9.43), it is possible to find a representation that is similar to the Silberstein-Bateman form of the Maxwell's equations [38]. For this purpose, we introduce a vector column $\psi(t, \boldsymbol{p}) = (\boldsymbol{m}_{\boldsymbol{p}}, \boldsymbol{l}_{\boldsymbol{p}})^T$, which allows us to rewrite the equations of motion for the spin waves in the form (9.9), where the matrix in the right-hand side is now given by

$$\mathcal{H}_{\rm m} = \begin{pmatrix} 0 & -\varepsilon_{\boldsymbol{p}}^{(l)}(\hat{\boldsymbol{S}}\cdot\boldsymbol{n}) \\ -\varepsilon_{\boldsymbol{p}}^{(m)}(\hat{\boldsymbol{S}}\cdot\boldsymbol{n}) & 0 \end{pmatrix}. \tag{9.44}$$

Here, we omit damping terms, which we discuss later. In this form, the equations of motion for the spin waves resemble the Maxwell's equations in a dispersive medium where the roles of the electric permittivity and magnetic permeability is played by $\varepsilon_{\boldsymbol{p}}^{(m)}$ and $\varepsilon_{\boldsymbol{p}}^{(l)}$.

The matrix in (9.44) can be symmetrized by an appropriate choice of the units that can be expressed in the form of the transformation $\psi = \mathcal{N}\bar{\psi}$, where $\mathcal{N} = \mathrm{diag}([\varepsilon_{\boldsymbol{p}}^{(m)}]^{-1/2}, [\varepsilon_{\boldsymbol{p}}^{(l)}]^{-1/2})$. In the symmetric units, the equation of motion for the antiferromagnetic spin waves is written as

$$i\frac{\partial\bar{\psi}(t,\boldsymbol{p})}{\partial t} = \mathcal{H}_0(\boldsymbol{p})\bar{\psi}(t,\boldsymbol{p}), \tag{9.45}$$

where the matrix on the right-hand side becomes symmetric

$$\mathcal{H}_0(\boldsymbol{p}) = \begin{pmatrix} 0 & -\omega_{\boldsymbol{p}}(\hat{\boldsymbol{S}}\cdot\boldsymbol{n}) \\ -\omega_{\boldsymbol{p}}(\hat{\boldsymbol{S}}\cdot\boldsymbol{n}) & 0 \end{pmatrix} = -\omega_{\boldsymbol{p}}\sigma_1 \otimes (\hat{\boldsymbol{S}}\cdot\boldsymbol{n}), \tag{9.46}$$

with $\omega_{\boldsymbol{p}} = \sqrt{\varepsilon_{\boldsymbol{p}}^{(m)}\varepsilon_{\boldsymbol{p}}^{(l)}}$.

This expression has a structure similar to $\mathcal{H}(\boldsymbol{p})$ in (9.12) for the Maxwell's equations. The important difference between $\mathcal{H}_0$ and $\mathcal{H}$ comes from their properties under spatial inversion ($\mathcal{P}$) and time-reversal ($\mathcal{T}$) transformations. For example, in the case of the time-reversal transformation, $\phi(t,\boldsymbol{p})$ in (9.9) transforms as $\mathcal{T}\phi(t,\boldsymbol{p}) \to \sigma_3\phi(-t,\boldsymbol{p})$. The Pauli matrix σ_3 appears on the right-hand side due to the different transformation properties of the electric and magnetic field with respect to $\mathcal{T}$. In contrast, both components of $\psi(t,\boldsymbol{p})$ are odd under $\mathcal{T}$, so that $\mathcal{T}\psi(t,\boldsymbol{p}) \to -\psi(-t,\boldsymbol{p})$. This means that if we want to transform from the spin wave dynamics to the electrodynamics, we should replace σ_1 in (9.46) with $\sigma_2 = i\sigma_1\sigma_3$ to ensure correct properties under the $\mathcal{PT}$ transformations.

9.3.2 *Nongeometric Symmetries for Spin-Wave Dynamics*

Formal analogy between the equations of motion for the antiferromagnetic spin waves and the Maxwell's equations enables us to generalize the concept of nongeometric symmetries. We may ask a question about all the transformations $\bar{\psi}(t,\boldsymbol{p}) \to \bar{\psi}'(t,\boldsymbol{p})$ that leave the equation of motion (9.45) invariant.

In order to find all such symmetries, one can repeat the steps of Sect. 9.2.1.1. First, we have to transform to the basis where $\mathcal{H}_0(\boldsymbol{p})$ is diagonal. For this purpose, we make a unitary transformation $\bar{\psi} = \mathcal{U}_\mathrm{m}\tilde{\psi}$, where the transformation matrix, $\mathcal{U}_\mathrm{m} = U_1 \otimes \hat{U}_\Lambda$, is given by the rotation matrix to the helicity basis in (9.14) (where $\boldsymbol{p}$ is replaced by $\boldsymbol{n}$) combined with the $SU(2)$ rotation in the subspace of $\boldsymbol{m}_{\boldsymbol{p}}$ and $\boldsymbol{l}_{\boldsymbol{p}}$

$$U_1 = \frac{1}{\sqrt{2}}\begin{pmatrix} 1 & 1 \\ -1 & 1 \end{pmatrix}. \tag{9.47}$$

The resulting equation of motion for $\tilde{\psi}$ is given by (9.45) with the diagonal matrix on the right-hand side

$$\tilde{\mathcal{H}}_0 = \mathcal{U}_{\mathrm{m}}^{\dagger}\mathcal{H}_0\mathcal{U}_{\mathrm{m}} = \mathrm{diag}(-\omega_{\boldsymbol{p}}, \omega_{\boldsymbol{p}}, 0, \omega_{\boldsymbol{p}}, -\omega_{\boldsymbol{p}}, 0). \tag{9.48}$$

This describes two antiferromagnetic spin waves with an energy dispersion $\omega_{\boldsymbol{p}}$ degenerate with respect to the two polarization states. In an antiferromagnet, magnetization precession is locked in the real space to the direction of $\boldsymbol{n}$, so that these polarization states correspond to left and right circular polarizations along the anisotropy axis. This is in contrast to electrodynamics, where we deal with real helicity—precession around the direction of wave vector $\boldsymbol{p}$.

Secondly, we have to find all the matrices Q that commute with $\tilde{\mathcal{H}}_0$, which can be done precisely in the same way as in (9.17). It should be mentioned that in the region $(\alpha - \alpha')p^2 \gg \beta$, antiferromagnetic spin waves have almost linear dispersion, $\omega_{\boldsymbol{p}} = c_s p$, where the velocity is given by $c_s = \gamma M_s\sqrt{\delta(\alpha - \alpha')}$. This fact gives them the appearance similar to the electromagnetic waves. However, we emphasize that the linear dispersion is not essential for our symmetry analysis.

What is important is that the eigenvalues of $\tilde{\mathcal{H}}_0$ are degenerate. This fact allows us find the eight-dimensional algebra of the symmetry transformations, which is isomorphic to invariance algebra of the Maxwell's equations. The generators of this algebra can be chosen as follows

$$\begin{aligned} &Q_1 = i\sigma_2 \otimes (\hat{\boldsymbol{S}} \cdot \boldsymbol{n})\hat{D}, && Q_2 = \sigma_1 \otimes \hat{I}, \\ &Q_3 = \sigma_3 \otimes (\hat{\boldsymbol{S}} \cdot \boldsymbol{n})\hat{D}, && Q_4 = i\sigma_2 \otimes \hat{D}, \\ &Q_5 = \sigma_0 \otimes (\hat{\boldsymbol{S}} \cdot \boldsymbol{n}), && Q_6 = \sigma_3 \otimes \hat{D}, \\ &Q_7 = \sigma_0 \otimes \hat{I}, && Q_8 = \sigma_1 \otimes (\hat{\boldsymbol{S}} \cdot \boldsymbol{n}), \end{aligned} \tag{9.49}$$

where $\hat{D} = 2[(\hat{\boldsymbol{S}} \cdot \boldsymbol{n}_\perp)^2 - \hat{I}_3\boldsymbol{n}_\perp^2]/n_\perp^2 - (\hat{\boldsymbol{S}} \cdot \boldsymbol{n})^2$, $\hat{I}_3 = \mathrm{diag}(0, 0, 1)$, and $\boldsymbol{n}_\perp = (n_1, n_2, 0)$. The interpretation of these basis elements is similar to that in (9.19). We have the unit element Q_7, Q_8 up to the factor of $\omega_{\boldsymbol{p}}$ coincides with $\mathcal{H}_0(\boldsymbol{p})$ and, therefore, commutes with all the other basis elements, and Q_5 generates rotations along $\boldsymbol{n}$.

Remarkably, Q_2 plays a role of the duality transformation of the electromagnetic field. It generates a continuous symmetry transformation, the Bogolyubov's rotation, in the subspace of $\boldsymbol{m}_{\boldsymbol{p}}$ and $\boldsymbol{l}_{\boldsymbol{p}}$

$$\boldsymbol{m}_{\boldsymbol{p}} \to \boldsymbol{m}'_{\boldsymbol{p}} = \boldsymbol{m}_{\boldsymbol{p}} \cosh\theta + \sqrt{\frac{\varepsilon_{\boldsymbol{p}}^{(l)}}{\varepsilon_{\boldsymbol{p}}^{(m)}}}\boldsymbol{l}_{\boldsymbol{p}} \sinh\theta, \tag{9.50}$$

$$\boldsymbol{l}_{\boldsymbol{p}} \to \boldsymbol{l}'_{\boldsymbol{p}} = \boldsymbol{l}_{\boldsymbol{p}} \cosh\theta + \sqrt{\frac{\varepsilon_{\boldsymbol{p}}^{(m)}}{\varepsilon_{\boldsymbol{p}}^{(l)}}}\boldsymbol{m}_{\boldsymbol{p}} \sinh\theta, \tag{9.51}$$

which leaves (9.42) and (9.43) invariant for any real parameter θ. Similar to the electrodynamics, we have an algebraic property $Q_2 Q_2 = Q_8$, which establishes a relation between the duality, the rotation symmetry along $\boldsymbol{n}$, and ∂_t.

9.3.3 Conserving Chirality of Spin Waves

The existence of the symmetry transformations makes possible a formulation of the conservation laws that correspond to these symmetries. Conserving quantities can be expressed in terms of bilinear forms similar to (9.21)

$$C = \frac{1}{2} \int d^3 p \psi^{\dagger}(t, \boldsymbol{p}) \rho Q \psi(t, \boldsymbol{p}), \tag{9.52}$$

where Q is a symmetry transformation, which can be expressed as a linear combination of Q_i ($i = 1, \ldots, 8$), and the measure $\rho = \mathrm{diag}(\varepsilon_{\boldsymbol{p}}^{(m)}, \varepsilon_{\boldsymbol{p}}^{(l)})$ is necessary for transforming from the symmetric representation of the equations of motions in (9.45) and (9.46) to the original units.

The conservation law for spin-wave chirality can be formulated similar to the expression for the optical zilch in Sect. 9.2.1.3. Since the rotation symmetry is preserved only along the direction of $\boldsymbol{n}$, we take the component of the spin wave momentum along this direction $\boldsymbol{p}_n = (\boldsymbol{p} \cdot \boldsymbol{n})\boldsymbol{n}$, and apply the conservation law in (9.52) for the symmetry transformation $p_n Q_5 = (\hat{\boldsymbol{S}} \cdot \boldsymbol{p}_n)$. As a result, the expression for conserving spin-wave chirality is given by

$$C_{\chi}^{(\mathrm{m})} = \frac{i}{2} \int d^3 p \left[\varepsilon_{\boldsymbol{p}}^{(m)} \boldsymbol{m}_{\boldsymbol{p}}^* \cdot (\boldsymbol{p}_n \times \boldsymbol{m}_{\boldsymbol{p}}) + \varepsilon_{\boldsymbol{p}}^{(l)} \boldsymbol{l}_{\boldsymbol{p}}^* \cdot (\boldsymbol{p}_n \times \boldsymbol{l}_{\boldsymbol{p}}) \right], \tag{9.53}$$

which is a direct analogue of the Lipkin's zilch for the electromagnetic field. In real space, the chirality density for spin waves can be written as

$$\rho_{\chi}^{(\mathrm{m})}(t, \boldsymbol{r}) = \frac{1}{2} \left(\nabla_n \boldsymbol{m} \cdot \frac{\partial \boldsymbol{l}}{\partial t} + \nabla_n \boldsymbol{l} \cdot \frac{\partial \boldsymbol{m}}{\partial t} \right), \tag{9.54}$$

where $\nabla_n = \boldsymbol{\nabla} \cdot \boldsymbol{n}$.

Physical meaning of $C_{\chi}^{(\mathrm{m})}$ becomes clear if we rewrite the expression (9.53) in terms of circularly polarized magnon operators. In this case, total spin wave chirality is determined by the difference between the number of left ($N_{\boldsymbol{p}}^{(R)}$) and right ($N_{\boldsymbol{p}}^{(R)}$) polarized magnons [38]

$$C_{\chi}^{(\mathrm{m})} = 2 \sum_{\boldsymbol{p}} p_n \omega_{\boldsymbol{p}} \left(N_{\boldsymbol{p}}^{(L)} - N_{\boldsymbol{p}}^{(R)} \right). \tag{9.55}$$

Similar expression exists for the Lipkin's zilch written in terms of the polarized photon modes [30]. For a monochromatic spin wave, $C_\chi^{(\mathrm{m})}$ becomes proportional to the spin angular momentum component along $\boldsymbol{n}$, which in terms of magnon number operators is given by $S^{(n)} = \sum_{\boldsymbol{p}} (N_{\boldsymbol{p}}^{(L)} - N_{\boldsymbol{p}}^{(R)})$ [30].

9.3.4 Spin-Wave Chirality in Dissipative Media

By now, we have established that spin waves in antiferromagnets can be characterized by the chiral invariant $C_\chi^{(\mathrm{m})}$, which is analogous to the Lipkin's zilch in optics. Similar to the optical case, we may ask a question: how can we make this chirality of the spin waves visible? To answer this question, we should look at the symmetries. Since $C_\chi^{(\mathrm{m})}$ is a pseudoscalar that is odd under $\mathcal{P}$ and even under $\mathcal{T}$, we have to break the same symmetries inside the antiferromagnet following the idea discussed in Sect. 9.2.2 for the light-matter interactions in chiral metamaterials.

Since our model in (9.40) is not chiral, we should provide some symmetry breaking mechanism. One interesting possibility of such mechanism that is relevant for spintronic applications is based on electron spin current [38]. The flow of spin angular momentum is odd under the spatial inversion and even under the time reversal transformation, therefore, its interaction with antiferromagnetic spin waves is able to provide the necessary symmetry breaking.

The microscopic mechanism beyond this symmetry breaking is as follows. Let us consider an electron spin current flowing along the magnetic ordering direction $\boldsymbol{n}$, which can be injected into an antiferromagnetic insulator film by a proximity effect or can be created in bulk metallic antiferromagnets. A pure spin current consists of a number of spin majority electrons ($\uparrow$) polarized along $\boldsymbol{n}$ flowing with the velocity $\boldsymbol{v}_s$ parallel to $\boldsymbol{n}$ balanced by the same amount of spin minority electrons ($\downarrow$) moving with the velocity $-\boldsymbol{v}_s$, so that the net electric charge transport is zero. Since the spin-wave dynamics is slow with respect to that of the electrons, the latter are able to exert a spin transfer torque on the magnetization dynamics via the Zhang-Li mechanism [58]. If the local s-d interactions between the electrons and sublattice magnetizations are in the exchange dominant regime [59], which means that we can neglect the intersublattice electron scattering, the spin majority (minority) electrons couple mostly to $\boldsymbol{M}_1$ ($\boldsymbol{M}_2$) sublattice magnetization. In this situation, the spin-$\uparrow$ electrons create the spin transfer torque acting mostly on the magnetization $\boldsymbol{M}_1$

$$\boldsymbol{\mathfrak{T}}_1 = -\frac{1}{M_s^2}\boldsymbol{M}_1 \times (\boldsymbol{M}_1 \times (\boldsymbol{v}_s \cdot \nabla)\boldsymbol{M}_1) - \frac{\xi}{M_s}\boldsymbol{M}_1 \times (\boldsymbol{v}_s \cdot \nabla)\boldsymbol{M}_1, \tag{9.56}$$

where the first (second) term is the adiabatic (non-adiabatic) torque component, and $\xi \lesssim 1$ is the dimensionless parameter [58, 59]. At the same time, spin-$\downarrow$ electron flow produce the spin transfer torque $\boldsymbol{\mathfrak{T}}_2 = -\boldsymbol{\mathfrak{T}}_1$ applied to $\boldsymbol{M}_2$. Therefore, a pure spin current in the exchange dominant regime of the electron-spin interaction is able

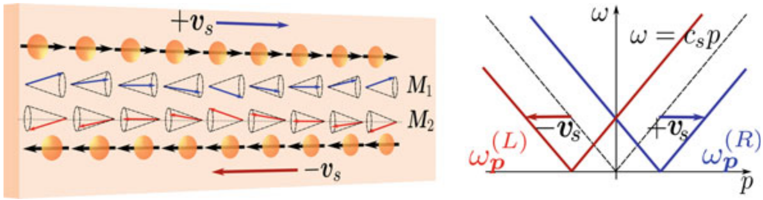

Fig. 9.2 Schematic picture of a pure spin current inside an antiferromagnet. Spin majority (minority) electrons moving with the velocity $+v_s$ ($-v_s$) create adiabatic spin torque applied to $\boldsymbol{M}_1$ ($\boldsymbol{M}_2$). These torques Doppler shift the energy dispersion of the left, $\omega_{\boldsymbol{p}}^{(L)}$, and right, $\omega_{\boldsymbol{p}}^{(R)}$, polarized modes in the opposite directions lifting the degeneracy between magnons of different polarizations

to create a pair of equal anti-parallel spin transfer torques $\mathfrak{T}_1$ and $\mathfrak{T}_2$ acting on magnetizations $\boldsymbol{M}_1$ and $\boldsymbol{M}_2$ respectively, as schematically shown in Fig. 9.2.

9.3.4.1 Doppler Shift from a Pure Spin Current

The Landau–Lifshitz–Gilbert equations of motion for the magnetizations in the presence of the spin-transfer torques are written as follows

$$\frac{\partial \boldsymbol{M}_1}{\partial t} = \gamma \boldsymbol{M}_1 \times \boldsymbol{H}_1^{\text{eff}} + \eta \boldsymbol{M}_1 \times \frac{\partial \boldsymbol{M}_1}{\partial t} - \frac{v_s}{M_s^2} \boldsymbol{M}_1 \times (\boldsymbol{M}_1 \times \nabla_n \boldsymbol{M}_1), \quad (9.57)$$

$$\frac{\partial \boldsymbol{M}_2}{\partial t} = \gamma \boldsymbol{M}_2 \times \boldsymbol{H}_2^{\text{eff}} + \eta \boldsymbol{M}_2 \times \frac{\partial \boldsymbol{M}_2}{\partial t} + \frac{v_s}{M_s^2} \boldsymbol{M}_2 \times (\boldsymbol{M}_2 \times \nabla_n \boldsymbol{M}_2), \quad (9.58)$$

where we neglect non-adiabatic contribution to the spin torque. Taking into account that $|\boldsymbol{M}_i| = M_s$ ($i = 1, 2$), these expressions can be rewritten as follows

$$\left(\frac{\partial}{\partial t} \mp v_s \nabla_n \right) \boldsymbol{M}_i = \gamma \boldsymbol{M}_i \times \boldsymbol{H}_i^{\text{eff}} + \eta \boldsymbol{M}_i \times \frac{\partial \boldsymbol{M}_i}{\partial t}, \quad (9.59)$$

where the upper (lower) sign is for $i = 1$ ($i = 2$). This expression shows that the role of the adiabatic spin transfer torque is to produce a Doppler shift of the spin waves by the velocity v_s. This effect is well-known for ferromagnetic and antiferromagnetic spin waves when the Doppler shift is caused by a spin polarized electric current [59–61]. In our case, the pure spin current produces two Doppler shifts in the opposite directions for the magnetization dynamics on each sublattice.

By solving the equations of motion (9.57) and (9.58), it is possible to show that in the presence of the spin current, the degeneracy between left and right polarizations in the dispersion relations for the spin waves propagating along $\boldsymbol{n}$ becomes lifted, and it can be approximated as follows [38]

$$\omega_{\boldsymbol{p}}^{(R)} = c_s|p - p_s| + i\eta(\Delta_s - pv_s), \tag{9.60}$$

$$\omega_{\boldsymbol{p}}^{(L)} = c_s|p + p_s| + i\eta(\Delta_s + pv_s), \tag{9.61}$$

where $p_s = \gamma M_s v_s \delta/(2c_s^2)$, $\Delta = \gamma M_s \delta/2$, and $p \gg p_s$ is the wave vector of the spin waves along $\boldsymbol{n}$, see Fig. 9.2.

This effect is in contrast to the Doppler shift from a spin polarized current where both modes are shifted in the same direction so that the degeneracy holds [59]. The imaginary parts of the frequencies $\omega_{\boldsymbol{p}}^{(R)}$ and $\omega_{\boldsymbol{p}}^{(L)}$ also have contributions from the spin current of the opposite signs for the waves with left and right polarizations. This can be considered as a spin-current-induced circular dichroims of spin waves, which occurs at the characteristic length scale $\ell_{\text{CD}} = c_s/(\eta v_s p)$.

Interestingly, the effect of spin current on the spin waves in the linear approximation is analogous to the existence of the additional Dzyaloshinskii-Moriya interaction (DMI) term in the antiferromagnetic energy in (9.40)

$$W_{\text{DMI}} = \frac{v_s}{2\gamma M_s} \int d^3r \left[\boldsymbol{m}_1 \cdot (\nabla_n \times \boldsymbol{m}_1) + \boldsymbol{m}_2 \cdot (\nabla_n \times \boldsymbol{m}_2)\right], \tag{9.62}$$

between the magnetizations on the same sublattices.

9.3.4.2 Asymmetric Energy Absorption

Let us now look at the spin-wave energy absorption. The dissipation rate for the magnetization dynamics can be expressed through the Rayleigh dissipation function

$$\frac{dW}{dt} = -\frac{\eta}{\gamma} \int d^3r \left[\left(\frac{\partial \boldsymbol{M}_1}{\partial t}\right)^2 + \left(\frac{\partial \boldsymbol{M}_2}{\partial t}\right)^2\right]. \tag{9.63}$$

According to the equations of motion (9.57) and (9.58), in the presence of the spin current we replace ∂_t with $\partial_t - v_s \nabla_n$ for $\boldsymbol{M}_1$ and with $\partial_t + v_s \nabla_n$ for $\boldsymbol{M}_2$. The energy dissipation rate in (9.63) in this case acquires the asymmetric contribution proportional to v_s that is written as

$$\left(\frac{dW}{dt}\right)_\chi = \frac{2\eta v_s}{\gamma} \int d^3r \left(\nabla_n \boldsymbol{m}_1 \cdot \frac{\partial \boldsymbol{m}_1}{\partial t} - \nabla_n \boldsymbol{m}_2 \cdot \frac{\partial \boldsymbol{m}_2}{\partial t}\right). \tag{9.64}$$

The expression in parentheses is nothing but the spin-wave chirality density $\rho_\chi^{(\text{m})}$ written in terms of $\boldsymbol{m}_1$ and $\boldsymbol{m}_2$.

As a result, when a pure spin current is injected into an antiferromagnet, the asymmetry in the spin-wave energy absorption rate becomes proportional to the spin-wave chirality, $(dW/dt)_\chi = 2\eta v_s \gamma^{-1} C_\chi^{\text{m}}$. This result is a direct analogy with the result of Tang and Cohen [27] for the electromagnetic energy absorption rate in chiral metamaterials, see Sect. 9.2.2. In antiferromagnetic materials, the microscopic mechanism beyond this phenomenon can be based on the adiabatic spin transfer torque from a pure spin current, or on the DMI between the same sublattices, which breaks the inversion symmetry and lifts the degeneracy between the left and right polarized magnon modes. In contrast to optical metamaterials, where the asymmetry in light-matter interactions is related to structural chirality, the symmetry breaking mechanism, which is based on the spin current, induces chirality of the material in controllable way. For a spin current density $j_s \approx 10^{11}$ A/m^2 (in the electric units), we obtain $v_s = \mu_B j_s/(eM_s) \approx 30$ m/s for $M_s \approx 3.5 \times 10^5$ A/m. This parameter should be compared to the typical velocity of the spin waves in antiferromagnetic insulators $c_s \approx 10^{-4}$ m/s, which gives $v_s/c_s \approx 10^{-3}$. The characteristic length of the magnon circular dichroism, in this situation, $\ell_{\rm CD} \approx 5$ mm for the magnon frequencies about 1 THz and $\eta \approx 10^4$. Curiously, the effective strength of the DMI, $D_{\rm eff} = \hbar v_s/(k_B a_0)$ is about 0.5 K (a_0 is the lattice spacing), which is comparable to a typical DMI strength in magnetic materials.

9.4 Excitation of Magnon Spin Photocurrents with Polarized Fields

Among the major goals of spintronics are generation of spin currents, their transmission over large distances, and conversion from one form to another because the spin angular momentum can be carried by different types of carriers. Since magnons are able to carry spin angular momentum, spin excitations in low damping magnetic insulators are good candidates for being spin current mediators. The absence of the net magnetization and the existence of two polarization states per magnon make antiferromagnetic insulators particularly suitable for applications as spin current conductors. It was demonstrated that an introduction of a thin layer of the antiferromagnetic insulator can enhance the spin current transmission in interface systems [62, 63].

Magnon spin currents in antiferromagnetic insulators can be excited by several methods. For example, it can be done by pumping a magnon spin current from a neighboring ferromagnetic layer [62]. Thermal excitation of spin currents via the spin versions of the Seebeck and Nernst effects also has attracted considerable attention [64–68]. The latter is especially interesting in low-dimensional materials, where it is provided by topological terms in magnon dynamics [69–71].

Optical control of spin states in antiferromagnetic insulators [72, 73] is a feature in the emerging field of antiferromagnetic optospintronics [5]. In this respect, it is an intriguing problem to investigate whether it is possible to find some sort of magnon photo-effect [44]. Symmetry considerations suggest that this is indeed possible. As we have already mentioned, spin currents satisfy the definition of true chirality [11], which can be directly seen from the conservation law for the μth component of the spin density

$$\frac{\partial s^\mu(t, \boldsymbol{r})}{\partial t} + \nabla \cdot \boldsymbol{j}^\mu(t, \boldsymbol{r}) = 0. \tag{9.65}$$

Since $s^{\mu}(t, \boldsymbol{r})$ is $\mathcal{T}$ odd and $\mathcal{P}$ even, the spin current density $\boldsymbol{j}^{\mu}(t, \boldsymbol{r})$ has opposite transformation properties. As we have seen in Sect. 9.2, the electromagnetic field can be characterized by optical chirality $\rho_{\chi}(t, \boldsymbol{r})$ with the same transformations properties as $\boldsymbol{j}^{\mu}(t, \boldsymbol{r})$. Therefore, we may expect that by exposing an antiferromagnetic insulator to a circularly polarized electromagnetic field, we can excite a spin photocurrent, which direction should be determined by the helicity of light.

In this section, we will consider these arguments in detail, and show that this photo-excitation process requires the frequency of the electromagnetic field to be in the region of the antiferromagnetic resonance. We begin with a semiclassical theory. Nonlinear response and geometric effects in low dimensional materials are discussed at the end of this section. First we consider an interesting phenomenon analogous to the *Zitterbewegung* effect for magnons.

9.4.1 Magnon Spin Currents in Antiferromagnets

Equations (9.42) and (9.43) preserve rotation symmetry along the magnetic ordering direction that warrants conservation of the total angular momentum component along $\boldsymbol{n}$. From these equations, the time evolution of the nth component of the magnetization $M^{(n)} = \frac{1}{2M_s}(m_2^2 - m_1^2)$ is written in the following form

$$\frac{\partial M^{(n)}(t, \boldsymbol{r})}{\partial t} = \frac{1}{4M_s} \sum_{\boldsymbol{pq}} e^{-i\boldsymbol{q}\cdot\boldsymbol{r}} \boldsymbol{n} \cdot \left\{ \left(\varepsilon^{(l)}_{\boldsymbol{p}-\boldsymbol{q}} - \varepsilon^{(l)}_{-\boldsymbol{p}} \right) \left[\boldsymbol{l}^*_{\boldsymbol{p}-\boldsymbol{q}} \times \boldsymbol{l}_{\boldsymbol{p}} \right] + \left(\varepsilon^{(m)}_{-\boldsymbol{p}+\boldsymbol{q}} - \varepsilon^{(m)}_{\boldsymbol{p}} \right) \left[\boldsymbol{m}^*_{\boldsymbol{p}-\boldsymbol{q}} \times \boldsymbol{m}_{\boldsymbol{p}} \right] \right\}. \tag{9.66}$$

In the limit $\boldsymbol{q} \to 0$, this equation can be rewritten in the form of a continuity equation $\partial_t M^{(n)}_{\boldsymbol{q}} + i\boldsymbol{q} \cdot \boldsymbol{J}^{(n)}_s = 0$, where

$$\boldsymbol{J}^{(n)}_s = \frac{i}{4M_s} \sum_{\boldsymbol{p}} \left(\frac{\partial \varepsilon^{(m)}_{\boldsymbol{p}}}{\partial \boldsymbol{p}} \boldsymbol{m}^*_{\boldsymbol{p}} \cdot (\boldsymbol{n} \times \boldsymbol{m}_{\boldsymbol{p}}) + \frac{\partial \varepsilon^{(l)}_{\boldsymbol{p}}}{\partial \boldsymbol{p}} \boldsymbol{l}^*_{\boldsymbol{p}} \cdot (\boldsymbol{n} \times \boldsymbol{l}_{\boldsymbol{p}}) \right) \tag{9.67}$$

is the total magnon spin current. This expression looks similar to our definition of the spin-wave chirality in (9.53), especially if we consider the spin current flow along $\boldsymbol{n}$. However, as we shall see below, in contrast to magnon chirality, $\boldsymbol{J}^{(n)}_s$ does not obey any conservation law. It should be mentioned that the same expression for the spin current can be obtained directly from the antiferromagnetic Lagrangian using Noether's theorem (see Appendix).

It is interesting to discuss the analogy between antiferromagnetic magnon spin currents and charge currents in pseudo-relativistic Dirac materials. In the latter case, it was demonstrated that interband effects make a significant contribution near the Dirac point and can explain, for example, the universal conductivity of graphene [74]. In the relativistic language, interband effects in the dynamics of an electron wave packet correspond to the *Zitterbewegung*, or the trembling motion of an ultra-relativistic particle [74]. The *Zitterbewegung* effect has also been proposed for antiferromagnetic magnons [40]. It can be easily understood by looking at the time evolution of $\bar{\psi}_{\boldsymbol{p}}(t)$ calculated from (9.45) to (9.46)

$$\bar{\psi}_{\boldsymbol{p}}(t) = \frac{1}{2}\left\{\left[1 + \sigma_1 \otimes (\hat{\boldsymbol{S}} \cdot \boldsymbol{n})\right] e^{i\omega_{\boldsymbol{p}} t} + \left[1 - \sigma_1 \otimes (\hat{\boldsymbol{S}} \cdot \boldsymbol{n})\right] e^{-i\omega_{\boldsymbol{p}} t}\right\} \bar{\psi}_{\boldsymbol{p}}(0), \quad (9.68)$$

which is similar to the analogous equation for relativistic particles [74]. This expression contains the off-diagonal elements responsible for the mixing of $\boldsymbol{m}_{\boldsymbol{p}}$ and $\boldsymbol{l}_{\boldsymbol{p}}$ components of $\bar{\psi}_{\boldsymbol{p}}$ while evolving in time.

By applying (9.68) to the time evolution of the spin current in (9.67), we find that the spin current has two contributions, $\boldsymbol{J}_s^{(n)}(t) = \boldsymbol{J}_{s0}^{(n)} + \boldsymbol{J}_{s1}^{(n)}(t)$. The first contribution is conserved part of the spin current. It does not depend on time and is proportional to the group velocity of magnons $v_{\boldsymbol{p}} = \partial\omega_{\boldsymbol{p}}/\partial\boldsymbol{p}$. In our matrix notations, it can be written as

$$\boldsymbol{J}_s^{(n)} = \frac{1}{4M_s}\sum_{\boldsymbol{p}} v_{\boldsymbol{p}} \bar{\psi}^{\dagger}(0)(\hat{\boldsymbol{S}} \cdot \boldsymbol{n})\bar{\psi}_{\boldsymbol{p}}(0). \quad (9.69)$$

The second term in the spin current oscillates at the double frequency, and can be attributed to the *Zitterbewegung* of magnons

$$\boldsymbol{J}_{s1}^{(n)}(t) = \frac{1}{16M_s}\sum_{\boldsymbol{p}} e^{2i\omega_{\boldsymbol{p}} t}\boldsymbol{K}_{\boldsymbol{p}} \bar{\psi}_{\boldsymbol{p}}^{\dagger}(0)\begin{pmatrix}(\hat{\boldsymbol{S}} \cdot \boldsymbol{n}) & 1 \\ -1 & -(\hat{\boldsymbol{S}} \cdot \boldsymbol{n})\end{pmatrix}\bar{\psi}_{\boldsymbol{p}}(0) + \text{H.c.}, \quad (9.70)$$

where

$$\boldsymbol{K}_{\boldsymbol{p}} = \frac{1}{\omega_{\boldsymbol{p}}}\left(\varepsilon_{\boldsymbol{p}}^{(l)}\frac{\partial\varepsilon_{\boldsymbol{p}}^{(m)}}{\partial\boldsymbol{p}} - \varepsilon_{\boldsymbol{p}}^{(m)}\frac{\partial\varepsilon_{\boldsymbol{p}}^{(l)}}{\partial\boldsymbol{p}}\right). \quad (9.71)$$

The physical meaning of these terms becomes clear if we transform to the helicity basis, $\tilde{\psi}_{\boldsymbol{p}} = (\tilde{\psi}_{\boldsymbol{p}}^{(R)}, \tilde{\psi}_{\boldsymbol{p}}^{(L)})^T$, where we have well-defined left and right polarized magnon modes, see (9.14), (9.47) and (9.48). In this basis, the first term is determined by the difference in numbers of magnons with opposite polarizations

$$\boldsymbol{J}_s^{(n)} = \frac{1}{4M_s}\sum_{\boldsymbol{p}} v_{\boldsymbol{p}}\left(\tilde{\psi}_{\boldsymbol{p}}^{*(R)}\tilde{\psi}_{\boldsymbol{p}}^{(R)} - \tilde{\psi}_{\boldsymbol{p}}^{*(L)}\tilde{\psi}_{\boldsymbol{p}}^{(L)}\right), \quad (9.72)$$

while the second term is purely off-diagonal and corresponds to the interband processes

$$\boldsymbol{J}_{s1}^{(n)}(t) = -\frac{1}{8M_s}\sum_{\boldsymbol{p}} \tilde{\psi}_{\boldsymbol{p}}^{\dagger}(0)\begin{pmatrix}0 & \boldsymbol{K}_{\boldsymbol{p}}\hat{S}^z e^{-2i\omega_{\boldsymbol{p}}\hat{S}^z t} \\ \boldsymbol{K}_{\boldsymbol{p}}\hat{S}^z e^{2i\omega_{\boldsymbol{p}}\hat{S}^z t} & 0\end{pmatrix}\tilde{\psi}_{\boldsymbol{p}}(0). \quad (9.73)$$

It should be mentioned that the contribution of the oscillating term in total spin current may seem insignificant. Indeed, in the theory the spin Seebeck effect only the term given by (9.72) was taken into account in the definition of the spin current [65, 66]. In this case, the second term, which mixes magnons of different helicities, has vanishing contribution. However, as we discuss below, such processes as the photo-excitation require both terms being considered with equal attention. Moreover, the contribution of the second term in (9.73) may become dominant in low-dimensional systems where it may contain geometric phase effects.

9.4.2 Photo-Excitation of Magnon Spin Currents

Let us now turn to a semi-classical theory of photo-excitation of magnon spin currents. For this purpose, we add a magneto-dipole interaction between the magnetic field component of the electromagnetic wave $\boldsymbol{h}(t, \boldsymbol{r})$ and the magnetization of the antiferromagnet, so that the total energy is written as

$$W_t = W - \int d^3r (\boldsymbol{M}_1 + \boldsymbol{M}_2) \cdot \boldsymbol{h}(t, \boldsymbol{r}), \tag{9.74}$$

where W is determined by (9.40). In this case, (9.43) acquires the additional term $-2\gamma M_s[\boldsymbol{n} \times \boldsymbol{h}_{\boldsymbol{p}}(t)]$, where $\boldsymbol{h}_{\boldsymbol{p}}(t)$ is the Fourier component of the magnetic field. The system of equations of motion (9.42) and (9.43) can be easily solved by transforming the ω-domain, which gives

$$\boldsymbol{m}_{\boldsymbol{p}}(\omega) = 2\gamma M_s \frac{\varepsilon_{\boldsymbol{p}}^{(l)} \boldsymbol{h}_{\boldsymbol{p}}(\omega)}{\omega_{\boldsymbol{p}}^2 - \omega^2}, \tag{9.75}$$

$$\boldsymbol{l}_{\boldsymbol{p}}(\omega) = 2i\gamma M_s \frac{\omega[\boldsymbol{n} \times \boldsymbol{h}_{\boldsymbol{p}}(\omega)]}{\omega_{\boldsymbol{p}}^2 - \omega^2}. \tag{9.76}$$

The Gilbert damping can be phenomenologically introduced in these equations by considering complex parameters $\varepsilon_{\boldsymbol{p}}^{(\alpha)} \to \varepsilon_{\boldsymbol{p}}^{(\alpha)} - i\eta\omega$ $(\alpha = m, l)$. Using the definition of the spin current in (9.67), we find the current excited by the magnetic field vector (Fig. 9.3)

$$\boldsymbol{J}_s^{(n)} = i\gamma^2 M_s \sum_{p\omega} \frac{\varepsilon_{\boldsymbol{p}}^{(l)2} \partial_{\boldsymbol{p}} \varepsilon_{\boldsymbol{p}}^{(m)} + \omega^2 \partial_{\boldsymbol{p}} \varepsilon_{\boldsymbol{p}}^{(l)}}{\left(\omega^2 - \omega_{\boldsymbol{p}}^2\right)^2} \boldsymbol{h}_{\boldsymbol{p}}^*(\omega) \cdot [\boldsymbol{n} \times \boldsymbol{h}_{\boldsymbol{p}}(\omega)]. \tag{9.77}$$

This expression shows that the direct spin current excited by the electromagnetic wave is the second order effect in $\boldsymbol{h}_{\boldsymbol{p}}(\omega)$, and is determined by the asymmetric combination $\boldsymbol{h}_{\boldsymbol{p}}^* \times \boldsymbol{h}_{\boldsymbol{p}}$, so that the direction of the current is determined by helicity of the electromagnetic wave. The effect is resonantly amplified near the antiferromagnetic resonance $\omega \approx \omega_{\boldsymbol{p}}$.

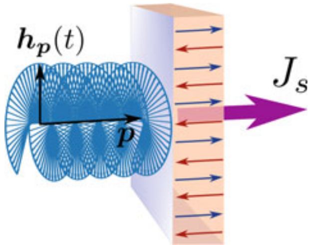

Fig. 9.3 Schematic picture of the magnon photocurrent $J_s^{(n)}$ induced inside an antiferromagnet by the circularly polarized electromagnetic wave propagating along the direction of magnetic ordering

Photo-excitation of magnon spin currents in antiferromagnetic insulators shows some similarity with the circular photogalvanic effect in noncentrosymmetric metals [45]. In the latter case, a direct electric photocurrent is generated by the helical combination the electric-field vector of the electromagnetic wave, $\boldsymbol{E}^*(\omega) \times \boldsymbol{E}(\omega)$, so that the direction of the current is reversed whenever circular polarization of light is switched to the opposite.

In order to have further insight into magnon spin photocurrents, let us consider a quantum variant of our theory.

9.4.3 Microscopic Theory of Magnon Spin Photocurrents

The spin Hamiltonian for an antiferromagnetic insulator with two magnetic sublattices A and B can be written in the following form

$$\hat{H} = \sum_{ij} \frac{1}{2} \left(J_{ij} S_i^{(+)} S_j^{(-)} + J_{ij}^* S_i^{(-)} S_j^{(+)} \right) + \sum_{ij} J'_{ij} S_i^z S_j^z - K \sum_i (S_i^z)^2, \qquad (9.78)$$

where J_{ij} and J'_{ij} are the exchange interaction constants such as $\mathrm{Re}\, J_{ij} > 0$ and $J'_{ij} > 0$ for the nearest neighboring sites on A and B sublattices, and $K \sim \beta a_0^{-3}$ is the magnetic anisotropy that stabilizes the antiferromagnetic ordering along the z direction. We do not specify any lattice configuration at this stage. However, we note that J_{ij} may have a complex phase factors in the presence of DMI.

The spin-wave approximation for the Hamiltonian (9.78) is conveniently expressed by the Holstein–Primakoff transformation of the spin operators

$$\begin{aligned} S_{iA}^{(+)} &= \sqrt{2S} a_i, \quad & S_{iB}^{(+)} &= \sqrt{2S} b_i^\dagger, \\ S_{iA}^{(-)} &= \sqrt{2S} a_i^\dagger, \quad & S_{iB}^{(-)} &= \sqrt{2S} b_i, \\ S_{iA}^z &= S - a_i^\dagger a_i, \quad & S_{iB}^z &= -S + b^\dagger b_i^\dagger, \end{aligned} \qquad (9.79)$$

where a_i and b_i are boson operators at the A and B sublattice respectively, which satisfy boson commutation relations. By transforming these operators to the reciprocal space, $a_i = \sum_{\boldsymbol{k}} \exp(i\boldsymbol{k} \cdot \boldsymbol{r}_i) a_{\boldsymbol{k}}$ and $b_i = \sum_{\boldsymbol{k}} \exp(i\boldsymbol{k} \cdot \boldsymbol{r}_i) b_{\boldsymbol{k}}$, we can rewrite (9.78) in the following form

$$\hat{H} = \sum_{\boldsymbol{k}} \left[A_{\boldsymbol{k}} \left(a^{\dagger}_{\boldsymbol{k}} a_{\boldsymbol{k}} + b^{\dagger}_{-\boldsymbol{k}} b_{-\boldsymbol{k}} \right) + B_{\boldsymbol{k}} a_{\boldsymbol{k}} b_{-\boldsymbol{k}} + B^{*}_{\boldsymbol{k}} a^{\dagger}_{\boldsymbol{k}} b^{\dagger}_{-\boldsymbol{k}} \right], \tag{9.80}$$

where parameters $A_{\boldsymbol{k}}$ and $B_{\boldsymbol{k}}$ include microscopic details. For example, in the case when the exchange interactions are limited by the nearest neighboring sites so that $J_{ij} = J^{'}_{ij} = J_1$, we obtain $A_{\boldsymbol{k}} = 2KS + ZJ_1S$ and $B_{\boldsymbol{k}} = J_1 S \sum_{\boldsymbol{\delta}} \exp(-i\boldsymbol{k} \cdot \boldsymbol{\delta})$, where $\boldsymbol{\delta}$ connects a site on the A sublattice with its Z nearest neighboring sites on the B sublattice.

9.4.3.1 Magnon Spin Currents: Quantum Version

The expression for a magnon spin current can be derived following the same steps as in Sect. 9.4.1. Considering the equation of motion for the z component of the local spin density, $n(\boldsymbol{r}_i) = b^{\dagger}_i b_i - a^{\dagger}_i a_i$, we find the total magnon spin current

$$\hat{\boldsymbol{J}}_s = \sum_{\boldsymbol{k}} \left[\frac{\partial A_{\boldsymbol{k}}}{\partial \boldsymbol{k}} \left(a^{\dagger}_{\boldsymbol{k}} a_{\boldsymbol{k}} + b^{\dagger}_{-\boldsymbol{k}} b_{-\boldsymbol{k}} \right) + \frac{\partial B_{\boldsymbol{k}}}{\partial \boldsymbol{k}} a_{\boldsymbol{k}} b_{-\boldsymbol{k}} + \frac{\partial B^{*}_{\boldsymbol{k}}}{\partial \boldsymbol{k}} a^{\dagger}_{\boldsymbol{k}} b^{\dagger}_{-\boldsymbol{k}} \right]. \tag{9.81}$$

This expression can be conveniently written in the matrix form

$$\hat{\boldsymbol{J}}_s = \sum_{\boldsymbol{k}} \chi^{\dagger}_{\boldsymbol{k}} \frac{\partial \mathcal{H}_{\boldsymbol{k}}}{\partial \boldsymbol{k}} \chi_{\boldsymbol{k}}, \tag{9.82}$$

where we introduced $\chi_{\boldsymbol{k}} = \begin{pmatrix} a_{\boldsymbol{k}} \\ b^{\dagger}_{-\boldsymbol{k}} \end{pmatrix}$ and $\mathcal{H}_{\boldsymbol{k}} = \begin{pmatrix} A_{\boldsymbol{k}} & B^{*}_{\boldsymbol{k}} \\ B_{\boldsymbol{k}} & A_{\boldsymbol{k}} \end{pmatrix}$. Note that in this representation, $\chi_{\boldsymbol{k}}$ does not satisfy boson communication relations; instead one has $[\chi_{\boldsymbol{k}}, \chi^{\dagger}_{\boldsymbol{k}'}] = \sigma_z \delta_{\boldsymbol{k},\boldsymbol{k}'}$, which should be kept in mind.

Let us find how $\hat{\boldsymbol{J}}_s$ transforms under the Bogolyubov's transformation that preserves boson commutation relations of magnon operators. In the matrix form, this transformation is expressed as $\chi_{\boldsymbol{k}} = U_{\boldsymbol{k}} \tilde{\chi}_{\boldsymbol{k}}$, where the transformation matrix is determined by two real parameters $\theta_{\boldsymbol{k}}$ and $\phi_{\boldsymbol{k}}$:

$$U_{\boldsymbol{k}} = \begin{pmatrix} \cosh \theta_{\boldsymbol{k}} e^{i\phi_{\boldsymbol{k}}} & -\sinh \theta_{\boldsymbol{k}} \\ -\sinh \theta_{\boldsymbol{k}} & \cosh \theta_{\boldsymbol{k}} e^{-i\phi_{\boldsymbol{k}}} \end{pmatrix}. \tag{9.83}$$

Since the definition of spin current involves $\partial_{\boldsymbol{k}}$, its transformation properties invoke covariant derivatives with respect to $U_{\boldsymbol{k}}$. Explicit calculations show that in an arbitrary basis

$$\hat{\boldsymbol{J}}_s = \sum_{\boldsymbol{k}} \tilde{\chi}^{\dagger}_{\boldsymbol{k}} \frac{\partial \tilde{\mathcal{H}}_{\boldsymbol{k}}}{\partial \boldsymbol{k}} \tilde{\chi}_{\boldsymbol{k}} - \frac{\partial \hat{\boldsymbol{A}}}{\partial t}, \tag{9.84}$$

where $\tilde{\mathcal{H}}_{\boldsymbol{k}} = U_{\boldsymbol{k}}^{\dagger}\mathcal{H}_{\boldsymbol{k}}U_{\boldsymbol{k}}$ is the Hamiltonian in the transformed basis, and $\hat{\boldsymbol{A}} = \sum_{\boldsymbol{k}} \tilde{\chi}_{\boldsymbol{k}}^{\dagger}\mathcal{A}_{\boldsymbol{k}}\tilde{\chi}_{\boldsymbol{k}}$ with

$$\mathcal{A}_{\boldsymbol{k}} = -i\sigma_z U_{\boldsymbol{k}}^{-1}\frac{\partial U_{\boldsymbol{k}}}{\partial \boldsymbol{k}} \tag{9.85}$$

being the connection associated with the transformation $U_{\boldsymbol{k}}$.

Among the various representations, there is one specific basis, where the Hamiltonian in (9.80) becomes diagonal. This basis is reached by choosing $\tanh 2\theta_{\boldsymbol{k}} = |B_{\boldsymbol{k}}|/A_{\boldsymbol{k}}$ and $\phi_{\boldsymbol{k}} = \arg B_{\boldsymbol{k}}$, which gives

$$\hat{H} = \sum_{\boldsymbol{k}} \varepsilon_{\boldsymbol{k}}\left(\alpha_{\boldsymbol{k}}^{\dagger}\alpha_{\boldsymbol{k}} + \beta_{-\boldsymbol{k}}^{\dagger}\beta_{-\boldsymbol{k}}\right), \tag{9.86}$$

where $\varepsilon_{\boldsymbol{k}} = \sqrt{A_{\boldsymbol{k}}^2 - |B_{\boldsymbol{k}}|^2}$ is the magnon energy dispersion. To find the expression for the spin current in this basis, we notice that in (9.84)

$$-\frac{\partial \hat{\boldsymbol{A}}}{\partial t} = i[\hat{\boldsymbol{A}}, \hat{H}] = \sum_{\boldsymbol{k}}(\alpha_{\boldsymbol{k}}^{\dagger}, \beta_{-\boldsymbol{k}})\begin{pmatrix} 0 & \boldsymbol{K}_{\boldsymbol{k}}^{*} \\ \boldsymbol{K}_{\boldsymbol{k}} & 0 \end{pmatrix}\begin{pmatrix} \alpha_{\boldsymbol{k}} \\ \beta_{-\boldsymbol{k}}^{\dagger} \end{pmatrix}, \tag{9.87}$$

is purely off-diagonal with $\boldsymbol{K}_{\boldsymbol{k}} = e^{i\phi_{\boldsymbol{k}}}\left[\varepsilon_{\boldsymbol{k}}^{-1}(A_{\boldsymbol{k}}\partial_{\boldsymbol{k}}|B_{\boldsymbol{k}}| - |B_{\boldsymbol{k}}|\partial_{\boldsymbol{k}}A_{\boldsymbol{k}}) - i|B_{\boldsymbol{k}}|\partial_{\boldsymbol{k}}\phi_{\boldsymbol{k}}\right]$. Therefore, the total magnon spin current is written as

$$\hat{\boldsymbol{J}}_s = \sum_{\boldsymbol{k}}(\alpha_{\boldsymbol{k}}^{\dagger}, \beta_{-\boldsymbol{k}})\begin{pmatrix} \boldsymbol{v}_{\boldsymbol{k}} & \boldsymbol{K}_{\boldsymbol{k}}^{*} \\ \boldsymbol{K}_{\boldsymbol{k}} & \boldsymbol{v}_{\boldsymbol{k}} \end{pmatrix}\begin{pmatrix} \alpha_{\boldsymbol{k}} \\ \beta_{-\boldsymbol{k}}^{\dagger} \end{pmatrix}, \tag{9.88}$$

where $\boldsymbol{v}_{\boldsymbol{k}} = \partial_{\boldsymbol{k}}\varepsilon_{\boldsymbol{k}}$ is the group velocity of magnons [44]. This expression generalizes two contributions to the spin current in (9.72) and (9.73) identified earlier in our semi-classical approach.

9.4.3.2 Nonlinear Response Theory for Magnon Spin Photocurrents

By using semi-classical equations of motion in Sect. 9.4.2, we have already demonstrated that magnon spin photocurrent is the second order effect in the magnetic field of the electromagnetic wave. Here, we show how the process of photo-excitation can be described via the nonlinear response theory.

Considering interaction of magnons with the electromagnetic wave as a perturbation, we can express the excited spin current using the second-order Kubo formula [75]

$$\langle \hat{\boldsymbol{J}}_s(t)\rangle = -\sum_{\omega_1\omega_2}\int_{-\infty}^{t} dt_1 \int_{-\infty}^{t_1} dt_2 e^{\epsilon(t_1+t_2-t)} e^{i\omega_1 t_1 + i\omega_2 t_2} \times \left\langle \left[\left[\hat{\boldsymbol{J}}_s(t), \hat{H}_I^{(\omega_1)}(t_1) \right], \hat{H}_I^{(\omega_2)}(t_2) \right] \right\rangle, \quad \epsilon \to 0^+, \quad (9.89)$$

where the interacting part of the Hamiltonian is taken in the form of dipole interaction between the magnetic field vector $\mathfrak{B}_{\boldsymbol{k}}(\omega)$ and the local magnetization of the antiferromagnet, $\hat{H}_I = -g\mu_B \sum_i \mathfrak{B}(t, \boldsymbol{r}_i)(\boldsymbol{S}_{iA} + \boldsymbol{S}_{iB})$, where g is the Landé factor. In terms of magnon operators, it is expressed as

$$\hat{H}_I^{(\omega)} = -g\mu_B \sqrt{\frac{S}{2}} \sum_{\boldsymbol{k}} \left[\mathfrak{B}_{\boldsymbol{k}}^{(-)}(\omega) \left(a_{\boldsymbol{k}} + b_{-\boldsymbol{k}}^{\dagger} \right) + \text{H.c.} \right]. \quad (9.90)$$

In (9.89), the operators are in the Heisenberg picture, e.g. $\hat{H}_I^{(\omega_1)}(t_1) = \exp(i\hat{H}t_1)\hat{H}_I^{(\omega_1)} \exp(-i\hat{H}t_1)$, and the statistical average is with the density matrix of the noninteracting system $\rho_0 = \exp(-\hat{H}/k_B T)$.

Straightforward algebra shows that the spin current is calculated from (9.89) as follows [44]

$$\langle \hat{\boldsymbol{J}}_s(t)\rangle = \frac{1}{4}\sum_{\omega\boldsymbol{k}} \left[\frac{\boldsymbol{v}_{\boldsymbol{k}}\mu_{\boldsymbol{k}}}{(\varepsilon_{\boldsymbol{k}}-\omega)^2+\Gamma^2} + \frac{\boldsymbol{v}_{\boldsymbol{k}}\mu_{\boldsymbol{k}}}{(\varepsilon_{\boldsymbol{k}}+\omega)^2+\Gamma^2} + \frac{\lambda_{\boldsymbol{k}}\boldsymbol{K}_{\boldsymbol{k}}}{(\varepsilon_{\boldsymbol{k}}-\omega-i\Gamma)(\varepsilon_{\boldsymbol{k}}+\omega-i\Gamma)} + \frac{\lambda_{\boldsymbol{k}}^*\boldsymbol{K}_{\boldsymbol{k}}^*}{(\varepsilon_{\boldsymbol{k}}-\omega+i\Gamma)(\varepsilon_{\boldsymbol{k}}+\omega+i\Gamma)} \right] \boldsymbol{h}_{\boldsymbol{k}}^{(-)}(\omega)\boldsymbol{h}_{-\boldsymbol{k}}^{(+)}(-\omega), \quad (9.91)$$

where $\boldsymbol{h} = -g\mu_B\sqrt{2S}\mathfrak{B}$, $h^{(\pm)} = h^x \pm h^y$, and the coefficient are given by

$$\mu_{\boldsymbol{k}} = \frac{A_{\boldsymbol{k}} - |B_{\boldsymbol{k}}|\cos\phi_{\boldsymbol{k}}}{\sqrt{A_{\boldsymbol{k}}^2 - |B_{\boldsymbol{k}}|^2}}, \quad (9.92)$$

$$\lambda_{\boldsymbol{k}} = e^{-i\phi_{\boldsymbol{k}}} \left(\frac{A_{\boldsymbol{k}}\cos\phi_{\boldsymbol{k}} - |B_{\boldsymbol{k}}|}{\sqrt{A_{\boldsymbol{k}}^2 - |B_{\boldsymbol{k}}|^2}} - i\sin\phi_{\boldsymbol{k}} \right). \quad (9.93)$$

This expression contains two kinds of terms. The first is proportional to the group velocity of magnons, and, therefore, can be associated with actual motion of magnon wave packets. The second, proportional to $\boldsymbol{K}_{\boldsymbol{k}}$, is related to intersublattice dynamics; it contains the phase gradient, $\partial_{\boldsymbol{k}}\phi_{\boldsymbol{k}}$. This phase can be interpreted as an offset in dynamics of the magnetizations on A and B sublattices given by $a_{\boldsymbol{k}}(t) \sim \exp(i\varepsilon_{\boldsymbol{k}}t)$ and $b_{-\boldsymbol{k}}^{\dagger}(t) \sim \exp(i\varepsilon_{\boldsymbol{k}}t - i\phi_{\boldsymbol{k}})$ respectively. It may be accumulated as a result of the DMI combined with a specific lattice configuration [76], or be generated by the external electric field via the Aharonov-Casher effect [77, 78].

In the case when both $\boldsymbol{v}_{\boldsymbol{k}}$ and $\boldsymbol{K}_{\boldsymbol{k}}$ are odd under the transformation $\boldsymbol{k} \to -\boldsymbol{k}$, the spin current is determined by the asymmetric part of $\boldsymbol{h}_{\boldsymbol{k}}^{(-)}(\omega)\boldsymbol{h}_{-\boldsymbol{k}}^{(+)}(-\omega)$, which is proportional to $i[\boldsymbol{h}_{\boldsymbol{k}}^{*}(\omega) \times \boldsymbol{h}_{\boldsymbol{k}}(\omega)]_z$. In the limiting case $\Gamma \to 0$ and $\phi_{\boldsymbol{k}} = 0$, we can combine both kinds of terms in (9.91), which eventually gives

$$\langle \hat{\boldsymbol{J}}_s(t) \rangle = \frac{i}{2} \sum_{\omega \boldsymbol{k}} \frac{q_{\boldsymbol{k}}^2 \partial_{\boldsymbol{k}} p_{\boldsymbol{k}} - \omega^2 \partial_{\boldsymbol{k}} q_{\boldsymbol{k}}}{(\varepsilon_{\boldsymbol{k}}^2 - \omega^2)^2} [\boldsymbol{h}_{\boldsymbol{k}}^{*}(\omega) \times \boldsymbol{h}_{\boldsymbol{k}}(\omega)]_z, \tag{9.94}$$

where $p_{\boldsymbol{k}} = A_{\boldsymbol{k}} + |B_{\boldsymbol{k}}|$ and $q_{\boldsymbol{k}} = A_{\boldsymbol{k}} - |B_{\boldsymbol{k}}|$, which coincides with (9.77) obtained from the semi-classical equations of motion [44].

9.4.4 Magnon Spin Photocurrents in Antiferromagnetic Insulators and Low Dimensional Materials

We have demonstrated that in antiferromagnetic materials magnon spin currents contain intraband terms, proportional to the group velocity of magnons, and interband terms, which by analogy to the relativistic mechanics can be associated with the *Zitterbewegung* effect of magnons. The latter is proportional to the fast-oscillating factors, which makes these terms irrelevant as far as response to a static perturbation is concerned. For the thermal excitation of spin currents, for example, the antiferromagnetic spin current can be taken in the form of (9.72) [65, 69, 70].

The response to a dynamic perturbation is different. Since spin photocurrent is the second-order effect, the interband terms that oscillate at the double frequency should be taken into account together with the intraband contributions, so that the resulting response current is given by (9.94).

For practical applications, the most interesting frequency region is near the antiferromagnetic resonance, $\omega \approx \varepsilon_{\boldsymbol{k}}$. In this area, the response current is resonantly amplified and determined by the damping of the material. In the case of ballistic magnon transport, when $\varepsilon_{\boldsymbol{k}} \gg \Gamma$, we can replace $\omega - \varepsilon_{\boldsymbol{k}} \pm i\Gamma \to \pm i\Gamma$ and $\omega + \varepsilon_{\boldsymbol{k}} \pm i\Gamma \to 2\omega_r$ near the resonance ω_r. In this limit, the dominant contribution in (9.91) comes from the first term proportional to $\boldsymbol{v}_{\boldsymbol{k}}$

$$\langle \hat{J}_s \rangle_{\text{res}} \approx \frac{i q_{\boldsymbol{k}}}{4\hbar\omega_r} \frac{v_{\boldsymbol{k}}}{\Gamma^2} [\boldsymbol{h}^{*}(\omega_r) \times \boldsymbol{h}(\omega_r)]_z, \tag{9.95}$$

where we used monochromatic microwave field with $\boldsymbol{h}_{\boldsymbol{k}}(\omega)$ [44]. This expression allows to estimate the order of magnitude for the spin photocurrent excited with circularly polarized light as $\langle \hat{J}_s \rangle_{\text{res}} \approx \chi g^2 \mu_B^2 J_1 S^2 c_s I_B / (2a_0 c^2 \hbar \eta^2 \omega_r)$, where we take $\Gamma = \hbar\eta\omega_r$, $\chi = \pm$ denotes helicity of the wave, $I_B = |\mathfrak{B}(\omega_r)|^2$ is intensity, and linear magnon energy disperison is implied, $|v_{\boldsymbol{k}}| = c_s$. For a typical material with $c_s = 3 \times 10^4$ m/s, $J_s = 200$ K, $\omega_r = 3 \times 10^{13}$ s^{-1}, $\eta = 10^{-4}$, and $a_0 = 0.5$ nm, we

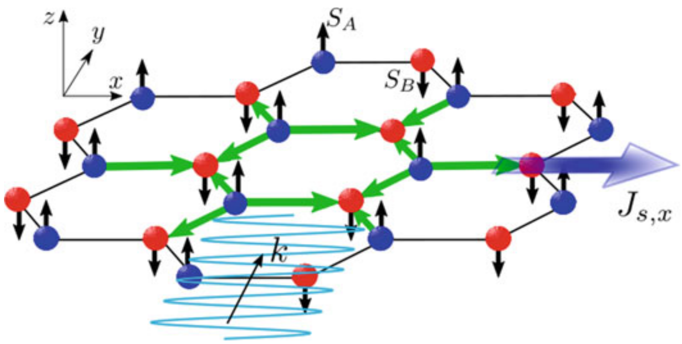

Fig. 9.4 Two-dimensional antiferromagnetic insulator with two magnetic sublattices $\boldsymbol{S}_A$ and $\boldsymbol{S}_B$ on the honeycomb lattice. Green arrows show the DMI configuration. The sign of D_{ij} is positive for $i \to j$ pointing from A to B

estimate $\langle \hat{J}_s \rangle_{\text{res}} \approx 1.5 \times 10^4$ A/m^2 (in electric units $e/\hbar$) for the microwave field strength $|\mathfrak{B}| \approx 10$ mT.

Relative contributions of different terms in (9.91) depend on the lattice configuration and on the details of microscopic interactions. We may expect that in low-dimensional antiferromagnets interband contribution determined by the phase gradient becomes more significant. We can separate this contribution from (9.91) as follows

$$\langle \hat{\boldsymbol{J}}_s \rangle_\phi = \frac{1}{2} \sum_{\omega \boldsymbol{k}} \frac{|B_{\boldsymbol{k}}| \sin \phi_{\boldsymbol{k}} \partial_{\boldsymbol{k}} \phi_{\boldsymbol{k}}}{\omega^2 - \varepsilon_{\boldsymbol{k}}^2} \boldsymbol{h}_{\boldsymbol{k}}^{(-)}(\omega) \boldsymbol{h}_{-\boldsymbol{k}}^{(+)}(-\omega). \tag{9.96}$$

Let us find a model system where this term in the spin current can be excited individually. For this purpose, we consider a two-dimensional antiferromagnet on the honeycomb lattice, as schematically shown in Fig. 9.4. This model is interesting because antiferromagnetic magnons on the honeycomb lattice have finite $\phi_{\boldsymbol{k}}$ even without DMI. Indeed, straightforward algebra shows that $B_{\boldsymbol{k}} = J_1 S C_{\boldsymbol{k}}$, where the structure factor is $C_{\boldsymbol{k}} = 2\cos(k_x/2)\cos(\sqrt{3}k_y/2) - 1 + 2i\sin(k_x/2)[\cos(k_x/2) - \cos(\sqrt{3}k_y/2)]$, which in the long-wavelength limit gives the phase $\phi_{\boldsymbol{k}} \approx k_x(3k_y^2 - k_x^2)/8$.

Note that $\phi_{\boldsymbol{k}}$ is odd under $\boldsymbol{k} \to -\boldsymbol{k}$. In order to break this symmetry, we add the specific DMI configuration $D_{ij}(\boldsymbol{S}_i \times \boldsymbol{S}_j)_z$ between the nearest neighboring sites i and j on the honeycomb lattice, such as $D_{ij} = D$ if $i \in A$ and $j \in B$, and $D_{ij} = -D$ otherwise. Adding such term does not modify the energy dispersion, but instead leads to the constant phase accumulation $B_{\boldsymbol{k}} = J_1 S C_{\boldsymbol{k}} \exp(i\phi_0)$ where $\tan \phi_0 = D/J_1$. In this case, $\sin(\phi_{\boldsymbol{k}} + \phi_0)\partial_{k_x}\phi_{\boldsymbol{k}}$ remains finite even in the $k_x \to 0$ limit. Therefore, by using (9.96), we are able to excite magnon spin current along x by the linearly polarized electromagnetic wave propagating along the y axis, see Fig. 9.4. The magnitude of the spin current is estimated as $\langle \boldsymbol{J}_s^x \rangle_\phi \approx 3g^2\mu_B^2 J_1 S/(8\hbar^2 c^2) \sin\phi_0 I_B \omega^2/(\omega^2 - \varepsilon_{\boldsymbol{k}}^2)$, and its sign is proportional to the sign of ϕ_0.

9.5 Conclusions

We have discussed how symmetry analysis can help to bring new ideas from optics to antiferromagnetic spintronics. Our discussion started with an observation that a formal similarity between the electromagnetic field and spin waves in an antiferromagnetic insulator allows to find a generalization of optical chirality. This forms a background for establishing a link between optics of chiral metamaterials and magnonics. For example, spin wave absorption in chiral antiferromagnets can be described in the same terms as the electromagnetic energy dissipation in metamaterials. Moreover, in antiferromagnets a pure spin current can provide a chiral symmetry breaking in a controllable way through the spin torque mechanism.

Fundamentally, this follows from the fact that spin currents are truly chiral; they have the same $\mathcal{PT}$ transformation properties as e.g. optical chirality density. The latter suggests that chiral electromagnetic fields can be used for magnon spin current generation. We discussed that a direct magnon spin current appears as a second-order response to the circularly polarized microwave field, which frequency is near the antiferromagnetic resonance. The direction of the current is determined by helicity of light that makes it similar to the circular photogalvanic effect in metals.

Lastly, we discuss how magnon spin currents in antiferromagnets have an interesting dynamics that can come into play for photo-excitation. Besides the transport terms proportional to the group velocity of the spin waves, there is a contribution from the trembling motion of magnons, which can be identified by analogy with motion of ultra-relativistic particles. Although these fast oscillating terms can be safely omitted in some applications, they contribute to the photo-excitation process.

Acknowledgements R.L.S. acknowledges the support of the Natural Sciences and Engineering Research Council of Canada (NSERC) RGPIN 05011-18.

Appendix: Magnon Spin Current Definition from the Antiferromagnetic Lagrangian

Let us consider a classical spin model for an antiferromagnet with two sublattices $\boldsymbol{S}_A$ and $\boldsymbol{S}_B$ with the energy given by

$$\mathcal{H}_{\text{AFM}} = J \sum_{\langle ij \rangle} \boldsymbol{S}_i \cdot \boldsymbol{S}_j - K \sum_i (S_i^z)^2, \tag{9.97}$$

where $J > 0$ is a nearest neighboring exchange interaction, K is the anisotropy constant along the z-axis, and summation is over the nearest neighboring sites on the A and B sublattices. For simplicity of notations, we consider one-dimensional arrangement of $\boldsymbol{S}_i$ along x. Semi-classical dynamics of this model can be captured from the following Lagrangian [79]

$$\mathcal{L} = \int dx \left[\rho \boldsymbol{M} \cdot \left(\boldsymbol{L} \times \frac{\partial \boldsymbol{L}}{\partial t} \right) - \frac{a}{2} |\boldsymbol{M}|^2 - A \frac{\partial}{\partial x} \left[\left(\frac{\partial \boldsymbol{L}}{\partial x} \right)^2 - \left(\frac{\partial \boldsymbol{M}}{\partial x} \right)^2 \right] - \ell \boldsymbol{M} \cdot \frac{\partial \boldsymbol{L}}{\partial x} + \frac{\tilde{\beta}}{2} (\boldsymbol{L}^z)^2 \right], \tag{9.98}$$

where $\boldsymbol{M} = \frac{1}{2S}(\boldsymbol{S}_A + \boldsymbol{S}_B)$ and $\boldsymbol{L} = \frac{1}{2S}(\boldsymbol{S}_A - \boldsymbol{S}_B)$, which satisfy the constraints $\boldsymbol{M} \cdot \boldsymbol{L} = 0$ and $\boldsymbol{M}^2 + \boldsymbol{L}^2 = 1$. The parameters of the Lagrangian are as follows: $\rho = 2\hbar S$, $a = 8JS^2$, $\ell = 2JS^2 a_0$, $A = JS^2 a_0^2$, and $\beta = 4KS^2$. Note that this expression contains so-called topological term proportional to ℓ, which breaks the inversion symmetry in the Lagrangian [79].

The expression for the spin current can be obtained applying the Noether's theorem to the Lagrangian transformation under the local infinitesimal rotation around z

$$\boldsymbol{M} \to \boldsymbol{M} + \delta\phi(\hat{z} \times \boldsymbol{M}), \tag{9.99}$$

$$\boldsymbol{L} \to \boldsymbol{L} + \delta\phi(\hat{z} \times \boldsymbol{L}), \tag{9.100}$$

where $\delta\phi(x)$ is the local rotation angle. The corresponding change in the Lagrangian is given by

$$\delta\mathcal{L} = -\int dx \delta\phi \left\{ \rho \frac{\partial}{\partial t} \left[M^z (1 - |\boldsymbol{M}|^2) \right] - A \frac{\partial}{\partial x} \left[(\hat{z} \times \boldsymbol{L}) \cdot \frac{\partial \boldsymbol{L}}{\partial x} - (\hat{z} \times \boldsymbol{M}) \cdot \frac{\partial \boldsymbol{M}}{\partial x} \right] - \ell \frac{\partial}{\partial x} \left[\boldsymbol{M} \cdot (\hat{z} \times \boldsymbol{L}) \right] \right\}, \tag{9.101}$$

which gives the following expression for the spin current density

$$j_s^z = -A\hat{z} \left[\left(\boldsymbol{L} \times \frac{\partial \boldsymbol{L}}{\partial x} \right) - \left(\boldsymbol{M} \times \frac{\partial \boldsymbol{M}}{\partial x} \right) \right] - \ell \hat{z} \cdot (\boldsymbol{L} \times \boldsymbol{M}). \tag{9.102}$$

The first term in this expression is consistent with the expression for the spin current obtained from the equations of motion. The second is the contribution from the topological terms, which has different symmetry. In particular, it changes the sign if we interchange $\boldsymbol{S}_A$ and $\boldsymbol{S}_B$.

References

1. I. Žutić, J. Fabian, S. Das Sarma, Rev. Mod. Phys. **76**, 323 (2004). https://doi.org/10.1103/RevModPhys.76.323
2. S.E. Thompson, S. Parthasarathy, Mater. Today **9**(6), 20 (2006). https://doi.org/10.1016/S1369-7021(06)71539-5

3. V. Baltz, A. Manchon, M. Tsoi, T. Moriyama, T. Ono, Y. Tserkovnyak, Rev. Mod. Phys. **90**, 015005 (2018). https://doi.org/10.1103/RevModPhys.90.015005
4. L. Šmejkal, Y. Mokrousov, B. Yan, A.H. MacDonald, Nat. Phys. **14**(3), 242 (2018). https://doi.org/10.1038/s41567-018-0064-5
5. P. Němec, M. Fiebig, T. Kampfrath, A.V. Kimel, Nat. Phys. **14**, 229 (2018)
6. M. Harder, C.M. Hu, Solid State Phys. **69**, 47 (2018). https://doi.org/10.1016/bs.ssp.2018.08.001
7. S.V. Kusminskiy (2019), p. 1911.11104
8. L. Kelvin, *Baltimore Lectures on Molecular Dynamics and the Wave Theory of Light* (CJ Clay & Sons, London, 1904)
9. L.D. Barron, Chirality **24**(11), 879 (2012). https://doi.org/10.1002/chir.22017
10. L. Barron, Chem. Phys. Lett. **123**(5), 423 (1986). https://doi.org/10.1016/0009-2614(86)80035-5
11. L.D. Barron, *Molecular Light Scattering and Optical Activity* (Cambridge University Press, 2004)
12. R. Naaman, D.H. Waldeck, Annu. Rev. Phys. Chem. **66**(1), 263 (2015). https://doi.org/10.1146/annurev-physchem-040214-121554
13. K. Michaeli, N. Kantor-Uriel, R. Naaman, D.H. Waldeck, Chem. Soc. Rev. **45**, 6478 (2016). https://doi.org/10.1039/C6CS00369A
14. R. Naaman, Y. Paltiel, D.H. Waldeck, Nat. Rev. Chem. **3**, 250 (2019). https://doi.org/10.1038/s41570-019-0087-1
15. D.M. Lipkin, J. Math. Phys. **5**(5), 696 (1964). https://doi.org/10.1063/1.1704165
16. M.G. Calkin, Am. J. Phys. **33**(11), 958 (1965). https://doi.org/10.1119/1.1971089
17. D. Zwanziger, Phys. Rev. **176**, 1489 (1968). https://doi.org/10.1103/PhysRev.176.1489
18. W.I. Fushchich, A.G. Nikitin, *Symmetries of Maxwell's Equations*. Mathematics and Its Applications (Springer, Netherlands, 1987)
19. I.Y. Krivskii, V.M. Simulik, Theor. Math. Phys. **80**(2), 864 (1989). https://doi.org/10.1007/BF01016113
20. I.Y. Krivskii, V.M. Simulik, Theor. Math. Phys. **80**(3), 912 (1989). https://doi.org/10.1007/BF01016183
21. G.N. Afanasiev, Y.P. Stepanovsky, Nuovo Cimento A **109**(3), 271 (1996). https://doi.org/10.1007/BF02731014
22. I. Bialynicki-Birula, *Coherence and Quantum Optics VII* (Springer, 1996), pp. 313–322
23. P.D. Drummond, Phys. Rev. A **60**(5), R3331 (1999)
24. P.D. Drummond, J. Phys. B: At. Mol. Opt. Phys. **39**(15), S573 (2006)
25. N.H. Ibragimov, Acta Appl. Math. **105**(2), 157 (2008). https://doi.org/10.1007/s10440-008-9270-y
26. M.V. Berry, J. Opt. A: Pure Appl. Opt. **11**(9), 094001 (2009), http://stacks.iop.org/1464-4258/11/i=9/a=094001
27. Y. Tang, A.E. Cohen, Phys. Rev. Lett. **104**, 163901 (2010). https://doi.org/10.1103/PhysRevLett.104.163901
28. K.Y. Bliokh, F. Nori, Phys. Rev. A **83**, 021803 (2011). https://doi.org/10.1103/PhysRevA.83.021803
29. S.M. Barnett, R.P. Cameron, A.M. Yao, Phys. Rev. A **86**, 013845 (2012). https://doi.org/10.1103/PhysRevA.86.013845
30. M.M. Coles, D.L. Andrews, Phys. Rev. A **85**, 063810 (2012). https://doi.org/10.1103/PhysRevA.85.063810
31. T.G. Philbin, Phys. Rev. A **87**, 043843 (2013). https://doi.org/10.1103/PhysRevA.87.043843
32. E. Hendry, T. Carpy, J. Johnston, M. Popland, R. Mikhaylovskiy, A. Lapthorn, S. Kelly, L. Barron, N. Gadegaard, M. Kadodwala, Nat. Nanotechn. **5**(11), 783 (2010)
33. Y. Tang, A.E. Cohen, Science **332**(6027), 333 (2011). https://doi.org/10.1126/science.1202817
34. M. Schäferling, D. Dregely, M. Hentschel, H. Giessen, Phys. Rev. X **2**, 031010 (2012). https://doi.org/10.1103/PhysRevX.2.031010

35. E. Hendry, R.V. Mikhaylovskiy, L.D. Barron, M. Kadodwala, T.J. Davis, Nano Lett. **12**(7), 3640 (2012). https://doi.org/10.1021/nl3012787
36. E.O. Kamenetskii, R. Joffe, R. Shavit, Phys. Rev. E **87**, 023201 (2013). https://doi.org/10.1103/PhysRevE.87.023201
37. A. Canaguier-Durand, J.A. Hutchison, C. Genet, T.W. Ebbesen, New J. Phys. **15**(12), 123037 (2013)
38. I. Proskurin, R.L. Stamps, A.S. Ovchinnikov, J.I. Kishine, Phys. Rev. Lett. **119**, 177202 (2017). https://doi.org/10.1103/PhysRevLett.119.177202
39. S.M. Barnett, New J. Phys. **16**(9), 093008 (2014), http://stacks.iop.org/1367-2630/16/i=9/a=093008
40. W. Wang, C. Gu, Y. Zhou, H. Fangohr, Phys. Rev. B **96**, 024430 (2017). https://doi.org/10.1103/PhysRevB.96.024430
41. L. Landau, E. Lifshitz, *Quantum Electrodynamics* (Pergamon Press, 1983)
42. B. Yan, C. Felser, Annu. Rev. Condens. Matter Phys. **8**(1), 337 (2017). https://doi.org/10.1146/annurev-conmatphys-031016-025458
43. A. Sekine, K. Nomura, Phys. Rev. Lett. **116**, 096401 (2016). https://doi.org/10.1103/PhysRevLett.116.096401
44. I. Proskurin, A.S. Ovchinnikov, J.I. Kishine, R.L. Stamps, Phys. Rev. B **98**, 134422 (2018). https://doi.org/10.1103/PhysRevB.98.134422
45. V. Belinicher, B.I. Sturman, Sov. Phys. Uspekhi **23**(3), 199 (1980)
46. F. de Juan, A.G. Grushin, T. Morimoto, J.E. Moore, Nat. Commun. **8**(1), 1 (2017)
47. R.P. Cameron, S.M. Barnett, New J. Phys. **14**(12), 123019 (2012), http://stacks.iop.org/1367-2630/14/i=12/a=123019
48. K.Y. Bliokh, A.Y. Bekshaev, F. Nori, New J. Phys. **15**(3), 033026 (2013), http://stacks.iop.org/1367-2630/15/i=3/a=033026
49. I. Fernandez-Corbaton, G. Molina-Terriza, Phys. Rev. B **88**, 085111 (2013). https://doi.org/10.1103/PhysRevB.88.085111
50. I. Proskurin, A.S. Ovchinnikov, P. Nosov, J.I. Kishine, New J. Phys. **19**(6), 063021 (2017). https://doi.org/10.1088/1367-2630/aa6acd
51. F.I. Fedorov, *Teorija girotropii* (Izd. Nauka i Technika, 1976)
52. J. Lekner, Pure Appl. Opt.: J. Eur. Opt. Soc. Part A **5**(4), 417 (1996)
53. K. Cho (2015)
54. D. Jaggard, A. Mickelson, C. Papas, Appl. Phys. **18**(2), 211 (1979)
55. S. Tomita, K. Sawada, A. Porokhnyuk, T. Ueda, Phys. Rev. Lett. **113**, 235501 (2014). https://doi.org/10.1103/PhysRevLett.113.235501
56. E.J. Post, *Formal Structure of Electromagnetics: General Covariance and Electromagnetics* (North-Holland Publishing Company, Amsterdam, 1962)
57. A.I. Akhiezer, V.G. Bar'yakhtar, S.V. Peletminskii, *Spin Waves* (North-Holland Publishing Company, Amsterdam, 1968)
58. S. Zhang, Z. Li, Phys. Rev. Lett. **93**, 127204 (2004). https://doi.org/10.1103/PhysRevLett.93.127204
59. Y. Yamane, J. Ieda, J. Sinova, Phys. Rev. B **94**, 054409 (2016). https://doi.org/10.1103/PhysRevB.94.054409
60. V. Vlaminck, M. Bailleul, Science **322**(5900), 410 (2008). https://doi.org/10.1126/science.1162843
61. A.C. Swaving, R.A. Duine, Phys. Rev. B **83**, 054428 (2011). https://doi.org/10.1103/PhysRevB.83.054428
62. H. Wang, C. Du, P.C. Hammel, F. Yang, Phys. Rev. Lett. **113**, 097202 (2014). https://doi.org/10.1103/PhysRevLett.113.097202
63. R. Khymyn, I. Lisenkov, V.S. Tiberkevich, A.N. Slavin, B.A. Ivanov, Phys. Rev. B **93**, 224421 (2016). https://doi.org/10.1103/PhysRevB.93.224421
64. S. Seki, T. Ideue, M. Kubota, Y. Kozuka, R. Takagi, M. Nakamura, Y. Kaneko, M. Kawasaki, Y. Tokura, Phys. Rev. Lett. **115**, 266601 (2015). https://doi.org/10.1103/PhysRevLett.115.266601

65. S.M. Rezende, R.L. Rodríguez-Suárez, A. Azevedo, Phys. Rev. B **93**, 014425 (2016). https://doi.org/10.1103/PhysRevB.93.014425
66. S.M. Rezende, R.L. Rodríguez-Suárez, A. Azevedo, Phys. Rev. B **93**, 054412 (2016). https://doi.org/10.1103/PhysRevB.93.054412
67. S.M. Wu, W. Zhang, A. KC, P. Borisov, J.E. Pearson, J.S. Jiang, D. Lederman, A. Hoffmann, A. Bhattacharya, Phys. Rev. Lett. **116**, 097204 (2016). https://doi.org/10.1103/PhysRevLett.116.097204
68. J. Holanda, D.S. Maior, O.A. Santos, L.H. Vilela-Leão, J.B.S. Mendes, A. Azevedo, R.L. Rodríguez-Suárez, S.M. Rezende, Appl. Phys. Lett. **111**(17), 172405 (2017). https://doi.org/10.1063/1.5001694
69. R. Cheng, S. Okamoto, D. Xiao, Phys. Rev. Lett. **117**, 217202 (2016). https://doi.org/10.1103/PhysRevLett.117.217202
70. V.A. Zyuzin, A.A. Kovalev, Phys. Rev. Lett. **117**, 217203 (2016). https://doi.org/10.1103/PhysRevLett.117.217203
71. Y. Shiomi, R. Takashima, E. Saitoh, Phys. Rev. B **96**, 134425 (2017). https://doi.org/10.1103/PhysRevB.96.134425
72. T. Satoh, S.J. Cho, R. Iida, T. Shimura, K. Kuroda, H. Ueda, Y. Ueda, B.A. Ivanov, F. Nori, M. Fiebig, Phys. Rev. Lett. **105**, 077402 (2010). https://doi.org/10.1103/PhysRevLett.105.077402
73. C. Tzschaschel, K. Otani, R. Iida, T. Shimura, H. Ueda, S. Günther, M. Fiebig, T. Satoh, Phys. Rev. B **95**, 174407 (2017). https://doi.org/10.1103/PhysRevB.95.174407
74. M.I. Katsnelson, Eur. Phys. J. B **51**(2), 157 (2006). https://doi.org/10.1140/epjb/e2006-00203-1
75. S.V. Tiablikov, *Methods in the Quantum Theory of Magnetism* (Springer, 2013)
76. M. Kawano, C. Hotta (2018), arXiv:1805.05872
77. K. Nakata, J. Klinovaja, D. Loss, Phys. Rev. B **95**, 125429 (2017). https://doi.org/10.1103/PhysRevB.95.125429
78. S. Owerre, J. Phys. Commun. **1**(2), 021002 (2017)
79. E.G. Tveten, T. Müller, J. Linder, A. Brataas, Phys. Rev. B **93**, 104408 (2016). https://doi.org/10.1103/PhysRevB.93.104408